

DRACO: Robust Distributed Training via Redundant Gradients

Lingjiao Chen, Hongyi Wang, Zachary Charles, Dimitris Papailiopoulos
University of Wisconsin-Madison

Abstract

Distributed model training is vulnerable to worst-case system failures and adversarial compute nodes, *i.e.*, nodes that use malicious updates to corrupt the global model stored at a parameter server (PS). To tolerate node failures and adversarial attacks, recent work suggests using variants of the geometric median to aggregate distributed updates at the PS, in place of bulk averaging. Although median-based update rules are robust to adversarial nodes, their computational cost can be prohibitive in large-scale settings and their convergence guarantees often require relatively strong assumptions.

In this work, we present DRACO, a scalable framework for robust distributed training that uses ideas from coding theory. In DRACO, each compute node evaluates redundant gradients that are then used by the parameter server to eliminate the effects of adversarial updates. We present problem-independent robustness guarantees for DRACO and show that the model it produces is identical to the one trained in the adversary-free setup. We provide extensive experiments on real datasets and distributed setups across a variety of large-scale models, where we show that DRACO is several times to orders of magnitude faster than median-based approaches.

1 Introduction

Distributed and parallel implementations of stochastic optimization algorithms have become the de facto standard in large-scale model training [LAP⁺14, RRWN11, ZCL15, AWD10, ABC⁺16, CLL⁺15, PGCC17, CSAK14]. Due to increasingly common malicious attacks, hardware and software errors [CL⁺99, KAD⁺07, BGS⁺17, CSX17], a nontrivial challenge in distributed machine learning is protecting against adversarial compute nodes and failures that may affect the training process and can bias or corrupt the end model. It is known that in these distributed setups even a single adversarial node can introduce arbitrary bias and inaccuracies to the end models [BGS⁺17].

A recent line of work [BGS⁺17, CSX17] studies this problem under a synchronous training setup, where a parameter server (PS) stores the model, and compute nodes evaluate gradient updates that are shipped to the PS and applied to the global model. The aforementioned studies suggest that instead of averaging the gradients—a standard aggregation technique—the PS can use a robust version of averaging, *i.e.*, the geometric median (GM). The advantage of median-based approaches is that they can be robust to up to a constant fraction of the compute nodes being adversarial [CSX17]. However, in settings with large amounts of data, the cost of computing the geometric median can dwarf the cost of computing a batch of gradients [BGS⁺17], rendering it impractical for distributed deployment. Furthermore, proofs of convergence for such systems require restrictive assumptions such as convexity, and need to be re-tailored to each different training algorithm. A scalable distributed training framework that is robust against adversaries and can be applied to a large family of training algorithms (*e.g.*, mini-batch SGD, GD, coordinate descent, SVRG, etc.) remains an open problem.

In this paper, we take a different route compared to median-based approaches and use ideas from coding theory to ensure robustness during distributed training. We present DRACO, a general distributed training framework that is robust against adversarial nodes and worst-case compute errors. We show that DRACO

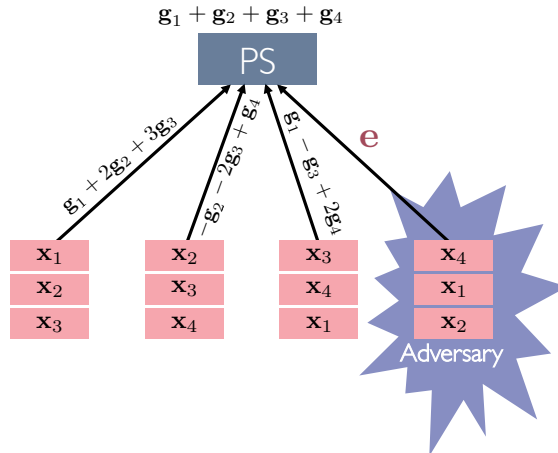


Figure 1: The high level idea behind DRACO’s algorithmic redundancy. Let us assume a data set consisting of 4 data points $\mathbf{x}_1, \dots, \mathbf{x}_4$, and let \mathbf{g}_i be the gradient of the model with respect to data point \mathbf{x}_i . In the present setup, instead of each compute node i evaluating a single gradient \mathbf{g}_i , during DRACO’s execution each node computes additional redundant gradients. In this example, the replication ratio is 3, and for the specific data allocation and gradient encoding mechanism shown above, the parameter server can recover the desired sum of gradients, *i.e.*, $\mathbf{g}_1 + \mathbf{g}_2 + \mathbf{g}_3 + \mathbf{g}_4$, from a linear combination of any 2 of the received encoded gradient updates. This means that in the presence of any single adversary, the PS can still recover the sum of the four gradients. This can be done through a majority vote on all $\binom{4}{2} = 6$ possible results from all pairs of encoded gradient updates. Although this is a simple decoding strategy, it cannot scale to a large number of compute nodes. DRACO implements a more systematic and efficient encoding and decoding mechanism that scales well on many machines.

can resist any s adversarial compute nodes during distributed training and it returns a model *identical* to the one trained in the adversary-free setup. This allows DRACO to come with “black-box” convergence guarantees, *i.e.*, proofs of convergence in the adversary-free setup carry through to the adversarial setup with no modification, unlike prior median-based approaches [BGS⁺17, CSX17]. Moreover, in median-based approaches such as [BGS⁺17, CSX17], computing the geometric median which is performed at the PS can dominate the overall training runtime. In DRACO most of the computational effort is carried through by the compute nodes. This is a key factor that allows our framework to offer up to orders of magnitude faster convergence in real distributed setups.

To design DRACO, we borrow ideas from coding theory and employ algorithmic redundancy. In standard adversary-free distributed computation setups, during each distributed round, each of the P compute nodes processes B/P gradients and ships their sum to the parameter server. In DRACO, each compute node processes rB/P gradients and sends a linear combination of those to the PS. This means that DRACO incurs a computational redundancy ratio of r . While this may seem sub-optimal, we show that under a worst-case adversarial setup, it is information theoretically impossible to design a system that obtains identical models to the adversary-free setup with less redundancy. Upon receiving the P gradient sums, the PS uses a “decoding” function to remove the effect of the adversarial nodes and reconstruct the original desired sum of the B gradients. With redundancy ratio r , we show that DRACO can tolerate up to $(r - 1)/2$ adversaries, which is information theoretically *tight*. See Fig. 1 for a toy example of DRACO’s functionality.

We present two constructions of encoding and decoding techniques that DRACO implements. The encoding schemes are based on the fractional repetition code and cyclic repetition codes presented in [TLDK17, RTTD17]. In contrast to previous work on stragglers and gradient codes [TLDK17, RTTD17, CPE17], our decoders are tailored to the adversarial setting and require different approaches. Our decoding schemes utilize an efficient majority vote style decoder and a novel Fourier decoding technique.

We note that compared to median-based techniques that can tolerate approximately a constant fraction

of “average case” adversaries, DRACO’s $(r - 1)/2$ bound on the number of “worst-case” adversaries can be significantly smaller. However, in realistic regimes where only a constant number of nodes are malicious, DRACO is significantly faster as we show in experiments in Section 4.

We implement DRACO in PyTorch and deploy it on distributed setups on Amazon EC2, where we compare against median-based training algorithms on several real world datasets and various ML models. We show that DRACO is up to orders of magnitude faster compared to GM-based approaches across a range of neural networks, *e.g.*, LeNet, VGG-19, AlexNet, ResNet-18, and ResNet-152, and always converges to the correct adversary-free model, while in some cases median-based approaches do not converge.

Related Work The large-scale nature of modern machine learning has spurred a great deal of novel research on distributed and parallel training algorithms and systems [RRWN11, DCM⁺12, AGL⁺17, JST⁺14, LWR⁺14, MPP⁺15, CPM⁺16]. A lot of this work has focused on developing and analyzing efficient implementations of distributed training algorithms. More recently, there has been interest in *federated learning* during which training is distributed among a large number of compute nodes (*e.g.*, edge devices), without centralized training data [KMR15, KMY⁺16, BIK⁺16].

In some of the above distributed setups, synchronous training can suffer from straggler nodes [ZKJ⁺08], where a few compute nodes are significantly slower than average. While early work on straggler mitigation used techniques similar to job replication [SLR16], more recent work has employed coding theory to speed up distributed machine learning systems [LLP⁺17, LMAA15, DCG16, DCG17, RPPA17]. Of particular note in this recent line of work is *gradient coding*, a straggler mitigation method proposed in [TLDK17], which uses codes to speedup synchronous distributed first-order methods such as mini-batch SGD [RTTD17, CPE17, CSSS11]. Our work builds on and extends this recent line of work to the adversarial setup. We note that mitigating stragglers is technically speaking a simpler problem compared to defending against adversarial nodes, since in the adversarial setup we have no knowledge as to which nodes are the adversaries.

The topic of byzantine fault tolerance has been extensively studied since the early 80s [LSP82]. A few recent studies focus on byzantine fault tolerance in the context distributed training, and show that while average-based gradient methods are susceptible to adversarial nodes [BGS⁺17, CSX17], median-based update methods can yield good convergence results while being robust to adversarial nodes. Both [BGS⁺17] and [CSX17] use variants of the geometric-median to improve the tolerance of first-order methods against adversarial nodes. Unfortunately, analyzing the convergence properties of median based approaches requires several assumptions and new proofs of convergence, as average based guarantees do not immediately transfer to the median setup. Furthermore, when the geometric median is used for aggregation, its computational cost can entirely dominate training time in large-scale settings.

We note that the idea of using redundancy to guard against failures in computational systems has existed for decades. Von Neumann used redundancy and majority vote operations in boolean circuits to achieve accurate computations in the presence of noise with high probability [VN56]. These results were further analyzed and extended in work such as [Pip88] to understand how susceptible a boolean circuit is to randomly occurring failures. Our work can be seen as an application of the aforementioned concepts to the context of distributed training in the face of adversity.

2 Preliminaries

Notation In the following, we will denote matrices and vectors in bold, and scalars and functions in standard script. We will let $\mathbf{1}_m$ denote the $m \times 1$ all ones vector, while $\mathbf{1}_{n \times m}$ will denote the all ones $n \times m$ matrix. We define $\mathbf{0}_m, \mathbf{0}_{n \times m}$ analogously.

Given a matrix $\mathbf{A} \in \mathbb{R}^{n \times m}$, we will let $\mathbf{A}_{i,j}$ denote its entry at location (i, j) . We will let $\mathbf{A}_{i,\cdot} \in \mathbb{R}^{1 \times m}$ denote its i th row, and $\mathbf{A}_{\cdot,j} \in \mathbb{R}^{n \times 1}$ will denote its j th column. Given $S \subseteq \{1, \dots, n\}, T \subseteq \{1, \dots, m\}$, we will let $\mathbf{A}_{S,T}$ denote the submatrix of \mathbf{A} where we keep rows indexed by S and columns indexed by T . Given matrices $\mathbf{A}, \mathbf{B} \in \mathbb{R}^{n \times m}$, their *Hadamard product*, denoted $\mathbf{A} \odot \mathbf{B}$, is defined as the $n \times m$ matrix where $(\mathbf{A} \odot \mathbf{B})_{i,j} = \mathbf{A}_{i,j} \mathbf{B}_{i,j}$.

Distributed Training The process of training a model from data can be cast as an optimization problem known as *empirical risk minimization* (ERM):

$$\min_{\mathbf{w}} \frac{1}{n} \sum_{i=1}^n \ell(\mathbf{w}; \mathbf{x}_i)$$

where $\mathbf{x}_i \in \mathbb{R}^m$ represents the i th data point, n is the total number of data points, $\mathbf{w} \in \mathbb{R}^d$ is a parameter vector or model, and $\ell(\cdot; \cdot)$ is a loss function that measures the accuracy of the predictions made by the model on each data point.

One way to approximately solve the above ERM is through stochastic gradient descent (SGD), which operates as follows. We initialize our parameter vector at an initial point \mathbf{w}_0 and then iteratively update it according to the rule

$$\mathbf{w}_k = \mathbf{w}_{k-1} - \gamma \nabla \ell(\mathbf{w}_{k-1}; \mathbf{x}_{i_k}),$$

where i_k is a random data-point index sampled from $\{1, \dots, n\}$, and $\gamma > 0$ is the learning rate.

In order to take advantage of distributed systems and parallelism, we often use *mini-batch* SGD instead. In this setup, at each iteration of the algorithm, we take a (possibly random) subset $S_k \subseteq \{1, \dots, n\}$ of the data and then update our model according to

$$\mathbf{w}_k = \mathbf{w}_{k-1} - \frac{\gamma}{|S_k|} \sum_{i \in S_k} \nabla \ell(\mathbf{w}_{k-1}; \mathbf{x}_i).$$

Many distributed versions of mini-batch SGD work by partitioning the gradient computations across the compute nodes in a distributed system. After computing their assigned gradients, the compute nodes then sum them up and send this sum back to the PS. The PS uses this sum of gradients to update the model \mathbf{w}_{k-1} according to the mini-batch SGD rule above.

In this work, we consider the question of how to perform each iteration of this update method in a distributed and robust manner. Since we consider a fixed iteration, we will fix some batch (or set of points) S_k , which after relabeling we assume equals $\{1, \dots, B\}$. We will denote $\nabla \ell(\mathbf{w}_{k-1}; \mathbf{x}_i)$ by \mathbf{g}_i . The fundamental question we consider in this work is how to compute $\sum_{i=1}^B \mathbf{g}_i$ in a distributed and *adversary-resistant* manner. We will present DRACO, a framework that can compute this summation in a distributed manner, even under the presence of adversaries.

Remark 1. *In contrast to previous works, our analysis and framework are applicable to any distributed algorithm which requires the sum of multiple functions. Notably, our framework can be applied to common first-order methods in machine learning, including gradient descent, variants of SGD, SVRG [JZ13], coordinate descent and various projected or accelerated versions of these algorithms. For the sake of simplicity, our discussion in the rest of the text will focus on mini-batch SGD.*

Adversarial Compute Node Model We consider the case where a subset of size s of the P compute nodes can act adversarially against the training process. It is known that mini-batch SGD fails to converge even if there is only a single adversarial node [BGS⁺17]. The goal of an adversary can either be to completely mislead the end model, or bias it towards specific areas of the parameter space. A compute node is considered to be an adversarial node, if it does not return the prescribed gradient update given its allocated samples. Such a node can ship back to the PS any arbitrary update of dimension equal to that of the true gradient.

In this work, we consider the strongest possible adversaries. We assume that in the worst-case an adversarial node has access to infinite computational power, has access to the entire data set and the training algorithm, and also has knowledge of what defense mechanism is used. Furthermore, all adversarial nodes may collaborate with each other.

3 DRACO: Robust Distributed Training via Algorithmic Redundancy

In this section we formally present our main results for DRACO. The proofs are left to the appendix.

We generalize the scheme in Figure 1 to P compute nodes and B data samples. At each iteration of our training process, we will assign the B gradients to the P compute nodes using a $P \times B$ allocation matrix \mathbf{A} . Here, $\mathbf{A}_{j,k}$ is 1 if node j is assigned the k th gradient \mathbf{g}_k , and 0 otherwise. Therefore, the support of $\mathbf{A}_{j,\cdot}$, denoted $\text{supp}(\mathbf{A}_{j,\cdot})$, is the set of indices k of gradients evaluated by the j th compute node. For simplicity, we will assume $B = P$ throughout the following.

DRACO utilizes redundant computations, so it is worth formally defining the amount of redundancy incurred. This is captured by the following definition.

Definition 1. The redundancy ratio r is defined by $r := \frac{1}{P} \|\mathbf{A}\|_0$.

In other words, the redundancy ratio is the average number of gradients assigned to each compute node.

We define a $d \times P$ matrix \mathbf{G} by $\mathbf{G} \triangleq [\mathbf{g}_1, \mathbf{g}_2, \dots, \mathbf{g}_P]$. In other words, \mathbf{G} has all assigned gradients as its columns. The j th compute node first computes a $d \times P$ gradient matrix $\mathbf{Y}_j \triangleq (\mathbf{1}_d \mathbf{A}_{j,\cdot}) \odot \mathbf{G}$ using its allocated gradients. In particular, if the k th gradient \mathbf{g}_k is allocated to the j th compute node, i.e., $\mathbf{A}_{j,k} \neq 0$, then the compute node computes \mathbf{g}_k as the k th column of \mathbf{Y}_j . Otherwise, it sets the k -th column of \mathbf{Y}_j to be $\mathbf{0}_d$.

The j th compute node is equipped with an encoding function E_j that maps the $d \times P$ matrix \mathbf{Y}_j of its assigned gradients to a single d -dimensional vector. After computing its assigned gradients, the j th compute node sends $\mathbf{z}_j \triangleq E_j(\mathbf{Y}_j)$ to the PS. If the j th node is adversarial then it instead sends $\mathbf{z}_j + \mathbf{n}_j$ to the PS, where \mathbf{n}_j is an arbitrary d -dimensional vector. We let E be the set of local encoding functions, i.e., $E = \{E_1, E_2, \dots, E_P\}$.

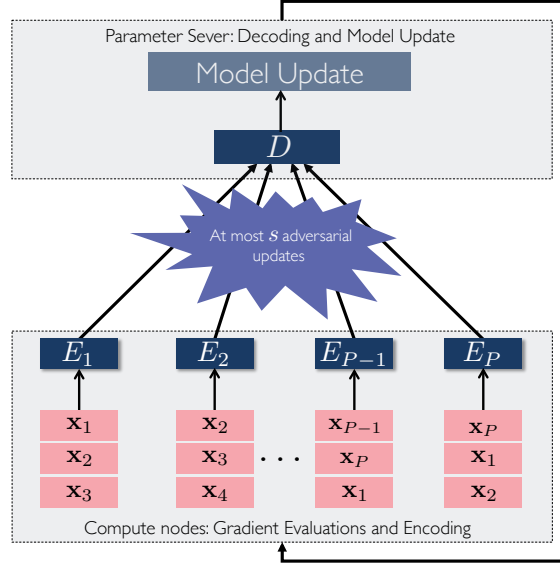


Figure 2: During DRACO each compute node is allocated a subset of the data set, in a systematic way that we define in Section 3. Each compute node will compute redundant gradients which will then be encoded by a local encoder function E_i . After encoding, each compute node sends an update vector to the parameter server. These received vectors then pass through a decoder that detects where the adversaries are and removes their effects from the updates. This way the output of the decoder is the full sum of the gradients originally intended to be received at the PS. The PS then applies the updates to the parameter model and the algorithm continues on to its next iteration.

We define a $d \times P$ matrix $\mathbf{Z}^{\mathbf{A},E,G}$ by $\mathbf{Z}^{\mathbf{A},E,G} \triangleq [\mathbf{z}_1, \mathbf{z}_2, \dots, \mathbf{z}_P]$, and we define a $d \times P$ matrix \mathbf{N} by $\mathbf{N} \triangleq [\mathbf{n}_1, \mathbf{n}_2, \dots, \mathbf{n}_P]$. Note that at most s columns of \mathbf{N} are non-zero.

Under this notation, after all updates are finished the PS receives a $d \times P$ matrix \mathbf{R} given by $\mathbf{R} \triangleq \mathbf{Z}^{\mathbf{A},E,G} + \mathbf{N}$. The PS then computes a single d -dimensional update gradient vector $\mathbf{u} \triangleq D(\mathbf{R})$ using some decoder function D .

The overall system in DRACO is therefore determined by the tuple (\mathbf{A}, E, D) . In other words, we get to choose how to assign gradients by designing \mathbf{A} , how each compute node should locally amalgamate its gradients by designing E , and how the PS should decode the output of all P compute nodes by designing D . The process of DRACO is illustrated in Figure 2.

This framework of (\mathbf{A}, E, D) encompasses both the framework of distributed SGD and the GM approach. For instance, in distributed mini-batch SGD, we assign 1 gradient to each compute node. After relabeling, we can assume that we assign \mathbf{g}_i to compute node i . Therefore, \mathbf{A} is simply the identity matrix \mathbf{I}_P . The matrix \mathbf{Y}_j therefore contains \mathbf{g}_j in column j and 0 in all other columns. The local encoding function E_j simply returns \mathbf{g}_j by computing $E_j(\mathbf{Y}_j) = \mathbf{Y}_j \mathbf{1}_P = \mathbf{g}_j$, which it then sends to the PS. The decoding function now depends on the algorithm. For vanilla mini-batch SGD, the PS takes the average of the gradients, while in the GM approach, it takes a geometric median of the gradients.

In order to guarantee convergence, we want to ensure that DRACO exactly recovers the desired gradient, regardless of the behavior of the adversarial nodes. In other words, we want DRACO to protect against *worst-case* adversaries. Formally, we want the PS to always obtain the sum of all gradients, i.e., the d -dimensional vector $\mathbf{G} \mathbf{1}_P$, via DRACO with any s adversarial nodes. A formal definition is given below.

Definition 2. DRACO with (\mathbf{A}, E, D) can tolerate s adversarial nodes, if for any $\mathbf{N} = [\mathbf{n}_1, \mathbf{n}_2, \dots, \mathbf{n}_P]$ such that $|\{j : \mathbf{n}_j \neq 0\}| \leq s$, we have $D(\mathbf{Z}^{\mathbf{A},E,G} + \mathbf{N}) = \mathbf{G} \mathbf{1}_P$.

Remark 2. Suppose that we can successfully defend against s adversaries. Then this means that after each distributed iteration we can recover the model update of the distributed algorithm as if we were under the adversary-free setup. This implies that any guarantees of convergence in the adversary-free case transfer to the adversarial case.

Redundancy Bound We first study how much redundancy is required if we want to exactly recover the correct sum of gradients per iteration in the presence of s adversaries. We give a lower bound on the amount of redundancy needed below.

Theorem 1. Suppose a selection of gradient allocation, encoding, and decoding mechanisms (\mathbf{A}, E, D) can tolerate s adversarial nodes. Then its redundancy ratio r must satisfy $r \geq 2s + 1$.

The above result is information theoretic, in the sense that it implies that regardless of how the compute node encodes and how the PS decodes, each data sample has to be replicated at least $2s + 1$ times to defend against s adversarial nodes.

Remark 3. Suppose that a selection of gradient allocation, encoding, and decoding mechanisms (\mathbf{A}, E, D) can tolerate any s adversarial nodes. By Theorem 1, this implies that on average, each compute node encodes at least $(2s + 1)$ d -dimensional vectors. Therefore, if the encoding has linear complexity, then each encoder requires $(2s + 1)d$ operations in the worst-case. If the decoder D has linear time complexity, then it requires at least Pd operations in the worst case, as it needs to use the d -dimensional input from all P compute nodes. This linear-time encoding and decoding gives a computational cost of $O(Pd)$ in general, which is significantly less than that of the GM approach in [BGS⁺17], which requires $O(P^2(d + \log P))$ operations.

Optimal Coding Schemes A natural question is, *can we achieve the optimal redundancy bound with linear-time encoding and decoding?* More formally, can we design a tuple (\mathbf{A}, E, D) that has redundancy ratio $r = 2s + 1$ and computation complexity $O((2s + 1)d)$ at the compute node and $O(Pd)$ at the PS? We give a positive answer by presenting two coding approaches that match the above bounds. The encoding methods are based on the fractional repetition code and the cyclic repetition codes in [TLDK17, RTTD17].

Fractional Repetition Code Suppose $2s + 1$ divides P . The fractional repetition code (derived from [TLDK17]) works as follows. We first divide all compute nodes into $r = 2s + 1$ groups. We assign the nodes in a group to each compute the same sum of gradients. Let $\hat{\mathbf{g}}$ denote the desired sum of gradients per iteration. In order to decode the outputs returned by the compute nodes in the same group, the PS uses majority vote to select one value. This guarantees that as long as fewer than half of the nodes in a group are adversarial, the majority procedure will return the correct $\hat{\mathbf{g}}$.

Formally, the repetition code $(\mathbf{A}^{Rep}, E^{Rep}, D^{Rep})$ is defined as follows. We will let \mathbf{A}^{Rep} be a block diagonal matrix whose diagonal elements are given by all $\mathbf{1}_{r \times r}$, i.e.,

$$\mathbf{A}^{Rep} = \begin{bmatrix} \mathbf{1}_{r \times r} & \mathbf{0}_{r \times r} & \mathbf{0}_{r \times r} & \cdots & \mathbf{0}_{r \times r} & \mathbf{0}_{r \times r} \\ \mathbf{0}_{r \times r} & \mathbf{1}_{r \times r} & \mathbf{0}_{r \times r} & \cdots & \mathbf{0}_{r \times r} & \mathbf{0}_{r \times r} \\ \vdots & \vdots & \vdots & \ddots & \ddots & \vdots \\ \mathbf{0}_{r \times r} & \mathbf{0}_{r \times r} & \cdots & \mathbf{0}_{r \times r} & \mathbf{0}_{r \times r} & \mathbf{1}_{r \times r} \end{bmatrix}.$$

The j th compute node first computes all its allocated gradients $\mathbf{Y}_j^{Rep} = (\mathbf{1}_d \mathbf{A}_{j,\cdot}^{Rep}) \odot \mathbf{G}$. Its encoder function simply takes the summation of all the allocated gradients. That is, $E_j^{Rep}(\mathbf{Y}_j^{Rep}) = \mathbf{Y}_j^{Rep} \mathbf{1}_P$. It then sends $\mathbf{z}_j = E_j^{Rep}(\mathbf{Y}_j^{Rep})$ to the PS.

The decoder works by first finding the majority vote of the output of each compute node that was assigned the same gradients. For instance, since the first r compute nodes were assigned the same gradients, it finds the majority vote of $[\mathbf{z}_1, \dots, \mathbf{z}_r]$. It does the same with each of the blocks of size r , and then takes the sum of the P/r majority votes. We note that our decoder here is different compared to the one used in the straggler mitigation setup of [TLDK17]. Our decoder follows the concept of majority decoding similarly to [VN56, Pip88].

Formally, D^{Rep} is given by $D^{Rep}(\mathbf{R}) = \sum_{\ell=1}^{\frac{P}{r}} Maj(\mathbf{R}_{\cdot, (\ell \cdot (r-1)+1):(\ell \cdot r)})$, where $Maj(\cdot)$ denotes the majority vote function and \mathbf{R} is the $d \times P$ matrix received from all compute nodes. While a naive implementation of majority vote scales quadratically with the number of compute nodes P , we instead use a streaming version of majority vote [BM91], the complexity of which is linear in P . Thus, the following result is obtained.

Theorem 2. *Suppose $2s + 1$ divides P . Then the repetition code $(\mathbf{A}^{Rep}, E^{Rep}, D^{Rep})$ with $r = 2s + 1$ can tolerate any s adversaries, achieves the optimal redundancy ratio, and has linear-time encoding and decoding.*

Cyclic Code Next we describe a cyclic code whose encoding method comes from [TLDK17] and is similar to that of [RTTD17]. We denote the cyclic code, with encoding and decoding functions, by $(\mathbf{A}^{Cyc}, E^{Cyc}, D^{Cyc})$. The cyclic code provides an alternative way to tolerate adversaries in distributed setups. We will show that the cyclic code also achieves the optimal redundancy ratio and has linear-time encoding and decoding. Another difference between the cyclic repetition code and the is that in the cyclic code, the compute nodes will compute and transmit complex vectors, and the decoding function will take as input these complex vectors.

To better understand the cyclic code, imagine that all P gradients we wish to compute are put in a circle. Since there are P starting positions, there are P possible ways to pick a sequence consisting of $2s + 1$ clock-wise consecutive gradients in the circle. Assigning each sequence of gradients to each compute node leads to redundancy ratio $r = 2s + 1$. Formally, its allocation matrix is

$$\mathbf{A}^{Cyc} = \begin{bmatrix} \overbrace{1 \ 1 \ \cdots \ 1}^{2s+1} \ 1 \ 0 \ 0 \ \cdots \ 0 \ 0 \\ 0 \ 1 \ 1 \ \cdots \ 1 \ 1 \ 0 \ \cdots \ 0 \ 0 \\ \vdots \ \vdots \ \vdots \ \vdots \ \vdots \ \ddots \ \ddots \ \vdots \ \vdots \\ 0 \ 0 \ \cdots \ 0 \ 0 \ 1 \ 1 \ \cdots \ 1 \ 1 \\ 1 \ 0 \ 0 \ \cdots \ 0 \ 0 \ 1 \ \cdots \ 1 \ 1 \\ \vdots \ \vdots \ \vdots \ \vdots \ \vdots \ \ddots \ \ddots \ \vdots \ \vdots \\ \underbrace{1 \ \cdots \ 1 \ 1}_{2s} \ 0 \ 0 \ \cdots \ 0 \ 0 \ 1 \end{bmatrix}.$$

In the cyclic code, each compute node computes a linear combination of its assigned gradients. This can be viewed as a generalization of the repetition code's encoder. Formally, we will construct some matrix $\mathbf{W} \in P \times P$ such that $\forall j, \ell, \mathbf{A}_{j,\ell}^{Cyc} \neq 0$ implies $\mathbf{W}_{j,\ell} = 0$. We then let $\mathbf{Y}_j^{Cyc} = (\mathbf{1}_d \mathbf{A}_{j,\cdot}^{Cyc}) \odot \mathbf{G}$ denote the gradients computed at compute node j . The local encoding function E_j^{Cyc} is defined by

$$\begin{aligned} E_j^{Cyc}(\mathbf{Y}_j^{Cyc}) &= \sum_{\ell: \|\mathbf{Y}_j^{Cyc}\|_{\cdot,\ell} \neq 0} \left[\mathbf{Y}_j^{Cyc} \right]_{\cdot,\ell} \mathbf{W}_{\ell,j} \\ &= \sum_{\ell=1}^n \left[\mathbf{Y}_j^{Cyc} \right]_{\cdot,\ell} \mathbf{W}_{\ell,j} \\ &= \mathbf{Y}_j^{Cyc} \mathbf{W}_{\cdot,j} \\ &= \mathbf{G} \mathbf{W}_{\cdot,j}. \end{aligned}$$

After performing this local encoding, the j th compute node then sends $\mathbf{z}_j^{Cyc} \triangleq E_j^{Cyc}(\mathbf{Y}_j^{Cyc})$ to the PS. Let $\mathbf{Z}^{\mathbf{A}^{Cyc}, \mathbf{E}^{Cyc}, \mathbf{G}} = [\mathbf{z}_1^{Cyc}, \mathbf{z}_2^{Cyc}, \dots, \mathbf{z}_P^{Cyc}]$. Then one can verify from the definition of E_j^{Cyc} that $\mathbf{Z}^{\mathbf{A}^{Cyc}, \mathbf{E}^{Cyc}, \mathbf{G}} = \mathbf{G} \mathbf{W}$. The received matrix at the PS now becomes $\mathbf{R}^{Cyc} = \mathbf{Z}^{\mathbf{A}^{Cyc}, \mathbf{E}^{Cyc}, \mathbf{G}} + \mathbf{N} = \mathbf{G} \mathbf{W} + \mathbf{N}$.

In order to decode, the PS needs to detect which compute nodes are adversarial and recover the correct gradient summation from the non-adversarial nodes. We note that methods to do the latter alone in the presence of straggler nodes was presented in [TLDK17] and [RTTD17]. Suppose there is a function $\phi(\cdot)$ that can compute the adversarial node index set V . We will later construct ϕ explicitly. Let U be the index set of the non-adversarial nodes. Suppose that the span of $\mathbf{W}_{\cdot,U}$ contains $\mathbf{1}_P$. Thus, we can obtain a vector \mathbf{b} by solving $\mathbf{W}_{\cdot,U} \mathbf{b} = \mathbf{1}_P$. Finally, since U is the index set of non-adversarial nodes, for any $j \in U$, we must have $\mathbf{n}_j = \mathbf{0}$. Thus, we can use $\mathbf{R}_{\cdot,U}^{Cyc} \mathbf{b} = (\mathbf{G} \mathbf{W} + \mathbf{N})_{\cdot,U} \mathbf{b} = \mathbf{G} \mathbf{W}_{\cdot,U} \mathbf{b} = \mathbf{G} \mathbf{1}_P$. The decoder function is given formally in Algorithm 1.

Algorithm 1 Decoder Function D^{Cyc} .

Input : Received $d \times P$ matrix \mathbf{R}^{Cyc}

Output: Desired gradient summation \mathbf{u}^{Cyc}

$V = \phi(\mathbf{R})$ // Locate the adversarial node indexes.

$U = \{1, 2, \dots, P\} - V$. // Non-adversarial node indexes

Find \mathbf{b} by solving $\mathbf{W}_{\cdot,U} \mathbf{b} = \mathbf{1}_P$

Compute and return $\mathbf{u}^{Cyc} = \mathbf{R}_{\cdot,U} \mathbf{b}$

In order to make this approach work, we need to design a matrix \mathbf{W} and the index location function $\phi(\cdot)$ such that (i) For all $j, k, \mathbf{A}_{j,k} = 0 \implies \mathbf{W}_{j,k} = 0$ and the span of $\mathbf{W}_{\cdot,U}$ contains $\mathbf{1}_P$, and (ii) $\phi(\cdot)$ can locate the adversarial nodes.

Let us first construct \mathbf{W} . Let \mathbf{C} be a $P \times P$ inverse discrete Fourier transformation (IDFT) matrix, i.e.,

$$\mathbf{C}_{jk} = \frac{1}{\sqrt{P}} \exp\left(\frac{2\pi i}{P}(j-1)(k-1)\right), \quad j, k = 1, 2, \dots, P.$$

Let \mathbf{C}_L be the first $P - 2s$ rows of \mathbf{C} and \mathbf{C}_R be the last $2s$ rows. Let α_j be the set of row indices of the zero entries in $\mathbf{A}_{\cdot,j}^{Cyc}$, i.e., $\alpha_j = \{k : \mathbf{A}_{j,k}^{Cyc} = 0\}$. Note that \mathbf{C}_L is a $(P - 2s) \times P$ Vandermonde matrix and thus any $P - 2s$ columns of it are linearly independent. Since $|\alpha_j| = P - 2s - 1$, we can obtain a $P - 2s - 1$ -dimensional vector \mathbf{q}_j uniquely by solving $\mathbf{0} = [\mathbf{q}_j \quad \mathbf{1}] \cdot [\mathbf{C}_L]_{\cdot,\alpha_j}$. Construct a $P \times (P - 2s - 1)$ matrix $\mathbf{Q} \triangleq [\mathbf{q}_1 \quad \mathbf{q}_2 \quad \dots \quad \mathbf{q}_P]$ and a $P \times P$ matrix $\mathbf{W} \triangleq [\mathbf{Q} \quad \mathbf{1}_P] \cdot \mathbf{C}_L$. One can verify that (i) each row of \mathbf{W} has the same support as the allocation matrix \mathbf{A}^{Cyc} and (ii) the span of any $P - 2s + 1$ columns of \mathbf{W} contains $\mathbf{1}_P$, summarized as follows.

Lemma 3. For all j, k , $\mathbf{A}_{j,k} = 0 \Rightarrow \mathbf{W}_{j,k} = 0$. For any index set U such that $|U| \geq P - (2s + 1)$, the column span of $\mathbf{W}_{\cdot,U}$ contains $\mathbf{1}_P$.

The $\phi(\cdot)$ function works as follows. Given the $d \times P$ matrix \mathbf{R}^{Cyc} received from the compute nodes, we first generate a $1 \times d$ random vector $\mathbf{f} \sim \mathcal{N}(\mathbf{1}_{1 \times d}, \mathbf{I}_d)$, and then compute $[h_{P-2s}, h_{P-2s-1}, \dots, h_{P-1}] \triangleq \mathbf{f} \mathbf{R}^{Cyc \dagger 1}$. We then obtain a vector $\beta = [\beta_0, \beta_1, \dots, \beta_{s-1}]^T$ by solving

$$\begin{bmatrix} h_{P-s-1} & h_{P-s} & \dots & h_{P-2} \\ h_{P-s-2} & h_{P-s-1} & \dots & h_{P-3} \\ \dots & \dots & \ddots & \vdots \\ h_{P-2s} & h_{P-s+1} & \dots & h_{P-s+1} \end{bmatrix} \begin{bmatrix} \beta_0 \\ \beta_1 \\ \vdots \\ \beta_{s-1} \end{bmatrix} = \begin{bmatrix} h_{P-1} \\ h_{P-2} \\ \vdots \\ h_{P-s} \end{bmatrix}.$$

We then compute $h_\ell = \sum_{u=0}^{s-1} \beta_u h_{\ell+u-s}$, where $\ell = 0, 1, \dots, P - 2s - 1$ and $h_\ell = h_{P+\ell}$. Once the vector $\mathbf{h} \triangleq [h_0, h_1, \dots, h_{P-1}]$ is obtained, we can compute the IDFT of \mathbf{h} , denoted by $\mathbf{t} \triangleq [t_0, t_1, \dots, t_{P-1}]$. The returned index set $V = \{j : t_{j+1} \neq 0\}$. The following lemma shows the correctness of $\phi(\cdot)$.

Lemma 4. Suppose $\mathbf{N} = [\mathbf{n}_1, \mathbf{n}_2, \dots, \mathbf{n}_P]$ satisfies $|\{j : \|\mathbf{n}_j\|_0 \neq 0\}| \leq s$. Then $\phi(\mathbf{R}^{Cyc} = \phi(\mathbf{G}\mathbf{W} + \mathbf{N}) = \{j : \|\mathbf{n}_j\|_0 \neq 0\}$ with probability 1.

Finally we can show that the cyclic code can tolerate any s adversaries and also achieves redundancy ratio and has linear-time encoding and decoding.

Theorem 5. The cyclic code $(\mathbf{A}^{Cyc}, \mathbf{E}^{Cyc}, \mathbf{D}^{Cyc})$ can tolerate any s adversaries with probability 1 and achieves the redundancy ratio lower bound. For $d \gg P$, its encoding and decoding achieve linear-time computational complexity.

Note that the cyclic code requires transmitting complex vectors $\mathbf{G}\mathbf{W}$ which potentially doubles the bandwidth requirement. To handle this problem, one can transform the original real gradient $\mathbf{G} \in \mathbb{R}^{d \times P}$ into a complex gradient $\hat{\mathbf{G}} \in \mathbb{C}^{\lceil d/2 \rceil \times P}$ by letting its i th component have real part \mathbf{G}_i and complex part $\mathbf{G}_{\lceil d/2 \rceil + i}$. Then the compute nodes only need to send $\hat{\mathbf{G}}\mathbf{W}$. Once the PS recovers $\hat{\mathbf{u}}^{Cyc} \triangleq \hat{\mathbf{G}}\mathbf{1}_P$, it can simply sum the real and imaginary parts to form the true gradient summation, i.e., $\mathbf{u}^{Cyc} = \text{Re}(\hat{\mathbf{u}}^{Cyc}) + \text{Im}(\hat{\mathbf{u}}^{Cyc}) = \mathbf{G}\mathbf{1}_P$.

4 Experiments

In this section we present an empirical study of DRACO and compare it to the median-based approach in [BGS⁺17] and [CSX17] under different adversarial models and real distributed environments. The main findings are as follows: 1) For the same training accuracy, DRACO is up to orders of magnitude faster compared to the GM-based approach; 2) In some instances, the GM approach [BGS⁺17, CSX17] does not converge, while DRACO converges in all of our experiments, regardless of which dataset, machine learning model, and adversary attack model we use; 3) Although DRACO is faster than GM-based approaches, its runtime can sometimes scale linearly with the number of adversaries due to the algorithmic redundancy needed to defend against adversaries.

Implementation and Setup We compare vanilla mini-batch SGD to both DRACO-based mini-batch SGD and GM-based mini-batch SGD [BGS⁺17, CSX17]. In mini-batch SGD, there is no data replication and each compute node only computes gradients sampled from its partition of the data. The PS then averages all received gradients and updates the model. In GM-based mini-batch SGD, the PS uses the geometric median instead of average to update the model. We have implemented all of those in PyTorch [PGC⁺17] with MPI4py [DPKC11] deployed on the m4.2/4/10xlarge instances in Amazon EC2. We conduct our experiments on various adversary attack models, datasets, learning problems and neural network models.

¹† denotes transpose conjugate.

Adversarial Attack Models We consider two adversarial models. First, we consider the “reversed gradient” adversary, where adversarial nodes that were supposed to send \mathbf{g} to the PS instead send $-\mathbf{c}\mathbf{g}$, for some $c > 0$. Next, we consider a “constant adversary” attack, where adversarial nodes always send a constant multiple κ of the all-ones vector to the PS with dimension equal to that of the true gradient. In our experiments, we set $c = 100$ for the reverse gradient adversary, and $\kappa = -100$ for the constant adversary. In either setup, at each iteration, s nodes are randomly selected to act as adversaries.

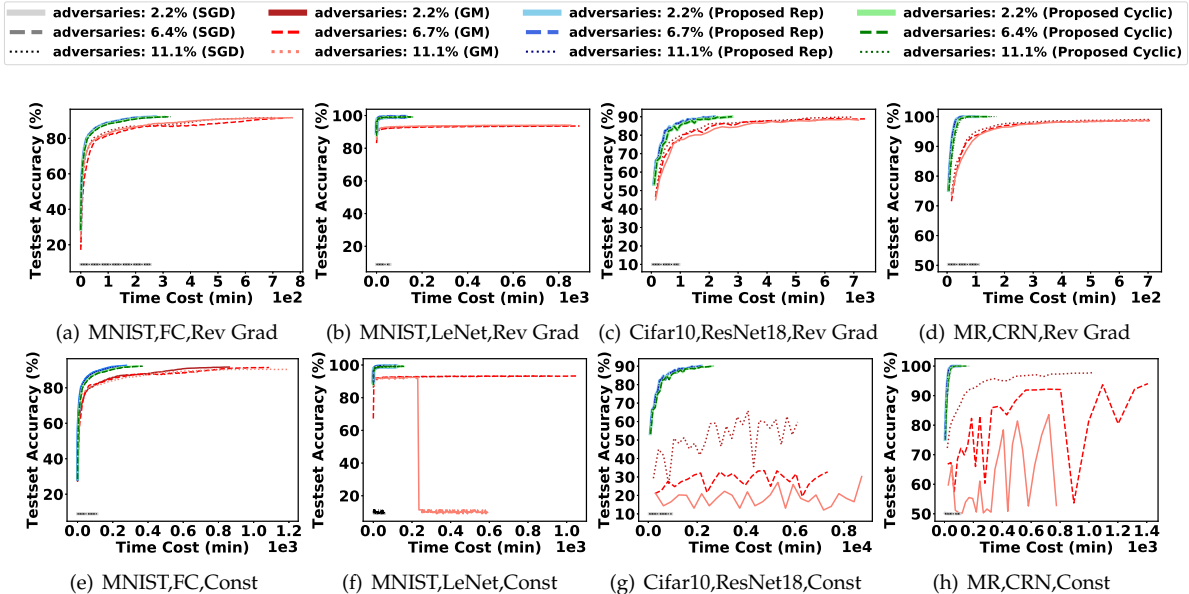


Figure 3: Convergence rates of DRACO, GM, and vanilla mini-batch SGD, on (a) MNIST on FC with reverse gradient adversaries, (b) MNIST on LeNet with reverse gradient adversaries, (c) Cifar10 on ResNet-18 with reverse gradient adversaries, (d) MR on CRN with reverse gradient adversaries, (e) MNIST on FC with constant adversaries, (f) MNIST on LeNet with constant adversaries, (g) Cifar10 on ResNet-18 with constant adversaries, and (h) MR on CRN with constant adversaries.

End-to-end Convergence Performance We first evaluate the end-to-end convergence performance of DRACO, using both the repetition and cyclic codes, and compare it to ordinary mini-batch SGD as well as the GM approach. The datasets and their associated learning models are summarized in Table 1. We use fully connected (FC) neural networks and LeNet [LBBH98] for MNIST, ResNet-18 [HZRS16] for Cifar 10 [KH09], and CNN-rand-non-static (CRN) model in [Kim14] for Movie Review (MR) [PL05].

The experiments were run on a cluster of 45 compute nodes instantiated on m4.2xlarge instances. At each iteration, we randomly select $s = 1, 3, 5$ (2.2%, 6.7%, 11.1% of all compute nodes) nodes as adversaries. All three methods are trained for 10,000 distributed iterations. Figure 3 shows how the testing accuracy varies with training time. Tables 2, 3, and 4 give a detailed account of the speedups of DRACO compared to the GM approach, where we run both systems until they achieve the same designated testing accuracy.

First, as expected, ordinary mini-batch may not converge even if there is only one adversary. Second, under the *reverse gradient adversary* model, DRACO converges several times faster than the GM approach, using both the repetition and cyclic codes. In fact, as shown in the speedup tables, both the repetition and the cyclic code versions of DRACO achieve up to more than an order of magnitude speedup compared to the GM approach. We suspect that this is because the computation of the GM is extremely expensive compared to the encoding and decoding overhead of DRACO.

Table 1: The datasets used, their associated learning models and corresponding parameters.

Dataset	MNIST	Cifar10	MR
# data points	70,000	60,000	10,662
Model	FC/LeNet	ResNet-18	CRN
# Classes	10	10	2
# Parameters	1,033k / 431k	1,1173k	154k
Optimizer	SGD	SGD	Adam
Learning Rate	0.01 / 0.01	0.1	0.001
Batch Size	720 / 720	180	180

Table 2: Speedups (*i.e.*, X times faster) of DRACO (Repetition/Cyclic Codes) over GM when using a fully-connected neural network on the MNIST dataset. We run both methods until they reach the same specified testing accuracy. In the table ‘const’ and ‘rev grad’ refer to the two types of adversarial updates.

Test Accuracy	80%	85%	88%	90%
2.2% const	3.4/2.7	3.5/2.8	4.8/3.9	4.1/3.1
6.7% const	2.7/2.0	4.1/3.1	6.0/4.6	5.6/4.1
11.1% const	2.9/2.2	4.8/3.7	6.1/4.7	5.3/3.8
2.2% rev grad	2.2/1.9	2.4/2.2	4.1/3.7	3.2/2.9
6.7% rev grad	3.1/2.5	3.3/3.1	5.5/4.8	4.5/3.7
11.1% rev grad	2.7/2.3	3.0/2.6	3.1/2.7	3.1/2.6

Table 3: Speedups of DRACO (with both repetition and cyclic codes) over GM when using ResNet-18 on Cifar10. We run both methods until they reach the same specified testing accuracy. Here ∞ means that the GM approach failed to converge to the same accuracy reached by DRACO.

Test Accuracy	80%	85%	88%	90%
2.2% rev grad	2.6/2.0	3.3/2.6	4.2/3.3	∞/∞
6.7% rev grad	2.8/2.2	3.4/2.7	4.3/3.4	∞/∞
11.1% rev grad	4.1/3.3	4.2/3.2	5.5/4.4	∞/∞

Table 4: Speedups of DRACO (with both repetition and cyclic codes) over GM when using CRM on MR. We run both methods until they reach the same specified testing accuracy.

Test Accuracy	95%	96%	98%	98.5%
2.2% rev grad	5.4/4.2	5.6/4.3	9.7/7.4	12/9.0
6.7% rev grad	6.4/4.5	6.3/4.5	11/8.1	19/13
11.1% rev grad	7.5/4.7	7.4/4.6	12/8	19/12

Under the *constant adversary* model, the GM approach sometimes failed to converge while DRACO still converged in all of our experiments. This reflects our theory, which shows that DRACO always returns a model identical to the model trained by the ordinary algorithm in an adversary-free environment. One reason why the GM approach may fail to converge is that by using the geometric median, it is actually losing information about a subset of the gradients. Under the constant adversary model, the PS effectively gains no information about the gradients computed by the adversarial nodes, and cannot recover the desired optimal model.

Another reason that GM may not converge may be because theoretical convergence guarantees of GM require certain assumptions on the underlying models, such as convexity. Since neural networks are generally non-convex, we have no guarantees that GM converges in these settings. It is worth noting that GM may also not converge if we were to use an algorithm such as L-BFGS or accelerated gradient descent, as the choice of algorithm is separate from the underlying properties of the neural network models. Nevertheless, DRACO still converges for such algorithms.

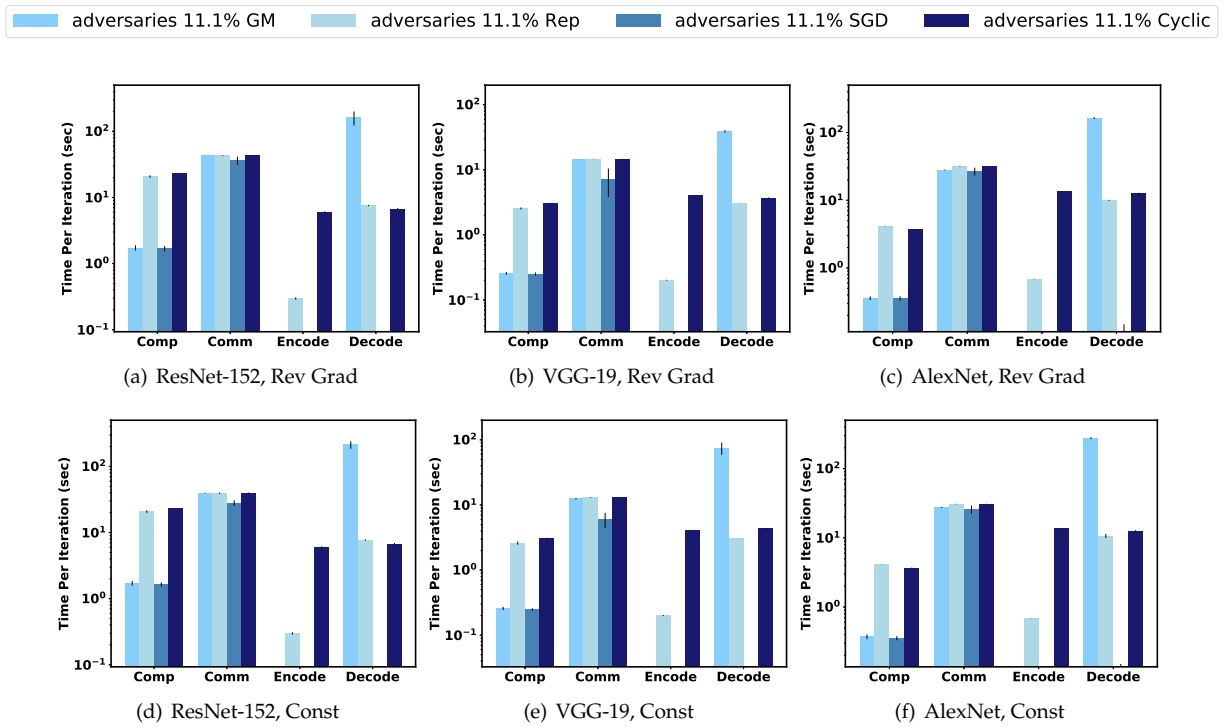


Figure 4: Empirical Per Iteration Time Cost on Large Models with 11.1% adversarial nodes (a): reverse gradient adversary on ResNet-152, (b): reverse gradient adversary on VGG-19, (c): reverse gradient adversary on AlexNet, (d): constant adversary on ResNet-152, (e): constant adversary on VGG-19, (f): constant adversary on AlexNet

Per iteration cost of DRACO We provide empirical per iteration costs of applying DRACO to three large state-of-the-art deep networks, ResNet-152, VGG-19, and AlexNet [HZRS16, SZ14, KSH12]. The experiments provided here are run on 46 real instances (45 compute nodes with 1 PS) on AWS EC2. For ResNet-152 and VGG-19, m4.4xlarge (equipped with 16 cores with 64 GB memory) instances are used while AlexNet experiments are run on m4.10xlarge (40 cores with 160 GB memory) instances given the high memory cost during training. We use a batch size of $B = 180$ and split the data among compute nodes. Therefore, each compute node is assigned $\frac{B}{n} = 4$ data points per iteration. We use the Cifar10 dataset for all the

aforementioned networks. For networks like AlexNet that were not designed for small images, we resize the Cifar10 images to fit the network. As shown in Figure 4, with $s = 5$, the encoding and decoding time of DRACO can be several times larger than the computation time of ordinary SGD, though SGD may not converge in adversarial settings. Nevertheless, DRACO is still several times faster than GM.

Table 5: Averaged Per Iteration Time Costs on ResNet-152 with 11.1% adversary

Time Cost (sec)	Comp	Comm	Encode	Decode
GM const	1.72	39.74	0	212.31
Rep const	20.81	39.36	0.24	7.74
SGD const	1.64	27.99	0	0.09
Cyclic const	23.08	39.36	5.94	6.64
GM rev grad	1.73	43.98	0	161.29
Rep rev grad	20.71	42.86	0.29	7.54
SGD rev grad	1.69	36.27	0	0.09
Cyclic rev grad	23.08	42.86	5.95	6.65

Table 6: Averaged Per Iteration Time Costs on VGG-19 with 11.1% adversary

Time Cost (sec)	Comp	Comm	Encode	Decode
GM const	0.26	12.47	0	74.63
Rep const	2.59	12.91	0.20	3.03
SGD const	0.25	6.9	0	0.03
Cyclic const	3.08	12.91	4.01	4.30
GM rev grad	0.26	14.57	0	39.02
Rep rev grad	2.55	14.66	0.20	3.04
SGD rev grad	0.25	7.15	0	0.03
Cyclic rev grad	3.07	14.66	4.02	3.65

Table 5, 6 and 7 provide the detailed cost of the runtime of each component of the algorithm in training ResNet-152, VGG-19 and AlexNet, respectively. While the communication cost is high in both DRACO and the GM method, the decoding time of the GM approach, i.e., its geometric median update at the PS, is prohibitively high. Meanwhile, the encoding and decoding overhead of DRACO is relatively negligible in these cases.

Effects of number of adversaries We also analyze how the number of adversaries affects the performance of DRACO. We ran Cifar10 on ResNet-18 with 15 compute nodes, varying the number of adversaries s from 1 to 7. For these experiments, we used the constant adversary model. For the repetition code, we adapted the group size based on s while in the cyclic code we always took $2s + 1$. Figure 5 shows the total runtime cost of DRACO does not increase significantly as the number of adversaries increase. This is likely due to the fact that even at $s = 7$, the communication cost (which is not affected by the number of stragglers) is the dominant cost of the algorithm.

Table 7: Averaged Per Iteration Time Costs on AlexNet with 11.1% adversarial nodes.

Time Cost (sec)	Comp	Comm	Encode	Decode
GM const	0.37	27.40	0	275.08
Rep const	4.16	30.71	0.67	10.65
SGD const	0.35	25.72	0	0.14
Cyclic const	3.67	30.71	13.55	12.54
GM rev grad	0.36	28.10	0	163.48
Rep rev grad	4.15	31.76	0.67	9.98
SGD rev grad	0.35	26.76	0	0.11
Cyclic rev grad	3.66	31.755	13.55	12.54

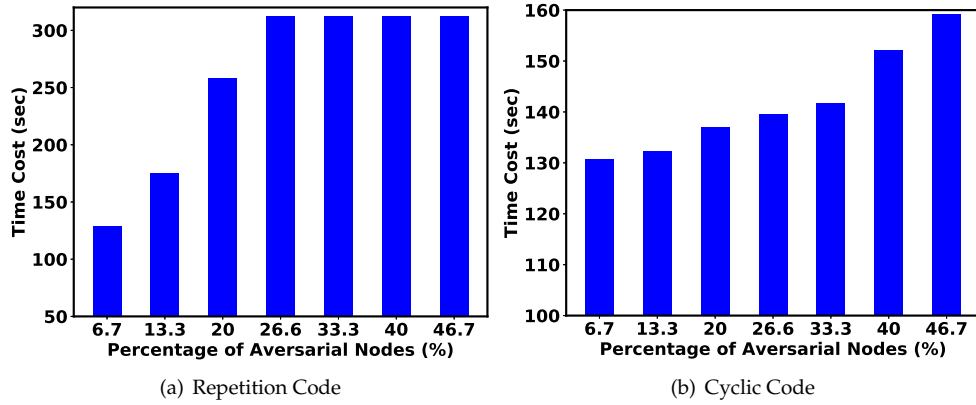


Figure 5: Time Cost to Reach 70% Test set Accuracy with Cifar10 dataset run with ResNet-18 on cluster 15 computation nodes varying Percentage of Adversarial Nodes from 6.7% to 46.7% with Constant Adversary (a) Repetition Code and (b) Cyclic Code

5 Conclusion and Open Problems

In this work we presented DRACO, a framework for robust distributed training via algorithmic redundancy. DRACO is robust to arbitrarily malicious compute nodes, while being orders of magnitude faster than state-of-the-art robust distributed systems. We give information-theoretic lower bounds on how much redundancy is required to resist adversaries while maintaining the correct update rule, and show that DRACO achieves this lower bound. There are several interesting future directions.

First, DRACO is designed to output the same model with or without adversaries. However, slightly inexact model updates often do not decrease performance noticeably. Therefore, we might ask whether we can either (1) tolerate more stragglers or (2) reduce the computational cost of DRACO by only *approximately* recovering the desired gradient summation. Second, while we give two relatively efficient methods for encoding and decoding, there may be others that are more efficient for use in distributed setups.

Acknowledgement

This work was supported in part by a gift from Google and AWS Cloud Credits for Research from Amazon. We thank Jeffrey Naughton and Remzi Arpacı-Dusseau for invaluable discussions and feedback on earlier drafts of this paper.

References

- [ABC⁺16] Martín Abadi, Paul Barham, Jianmin Chen, Zhifeng Chen, Andy Davis, Jeffrey Dean, Matthieu Devin, Sanjay Ghemawat, Geoffrey Irving, Michael Isard, et al. Tensorflow: A system for large-scale machine learning. In *OSDI*, volume 16, pages 265–283, 2016.
- [AGL⁺17] Dan Alistarh, Demjan Grubic, Jerry Li, Ryota Tomioka, and Milan Vojnovic. Qsgd: Communication-efficient sgd via gradient quantization and encoding. In *Advances in Neural Information Processing Systems*, pages 1707–1718, 2017.
- [AWD10] Alekh Agarwal, Martin J Wainwright, and John C Duchi. Distributed dual averaging in networks. In *Advances in Neural Information Processing Systems*, pages 550–558, 2010.
- [BGS⁺17] Peva Blanchard, Rachid Guerraoui, Julien Stainer, et al. Machine learning with adversaries: Byzantine tolerant gradient descent. In *Advances in Neural Information Processing Systems*, pages 118–128, 2017.
- [BIK⁺16] Keith Bonawitz, Vladimir Ivanov, Ben Kreuter, Antonio Marcedone, H Brendan McMahan, Sarvar Patel, Daniel Ramage, Aaron Segal, and Karn Seth. Practical secure aggregation for federated learning on user-held data. *arXiv preprint arXiv:1611.04482*, 2016.
- [BM91] Robert S Boyer and J Strother Moore. Mjrtv—a fast majority vote algorithm. In *Automated Reasoning*, pages 105–117. Springer, 1991.
- [CL⁺99] Miguel Castro, Barbara Liskov, et al. Practical byzantine fault tolerance. In *OSDI*, volume 99, pages 173–186, 1999.
- [CLL⁺15] Tianqi Chen, Mu Li, Yutian Li, Min Lin, Naiyan Wang, Minjie Wang, Tianjun Xiao, Bing Xu, Chiyuan Zhang, and Zheng Zhang. Mxnet: A flexible and efficient machine learning library for heterogeneous distributed systems. *arXiv preprint arXiv:1512.01274*, 2015.
- [CPE17] Zachary Charles, Dimitris Papailiopoulos, and Jordan Ellenberg. Approximate gradient coding via sparse random graphs. *arXiv preprint arXiv:1711.06771*, 2017.

- [CPM⁺16] Jianmin Chen, Xinghao Pan, Rajat Monga, Samy Bengio, and Rafal Jozefowicz. Revisiting distributed synchronous sgd. *arXiv preprint arXiv:1604.00981*, 2016.
- [CSAK14] Trishul M Chilimbi, Yutaka Suzue, Johnson Apacible, and Karthik Kalyanaraman. Project adam: Building an efficient and scalable deep learning training system. In *OSDI*, volume 14, pages 571–582, 2014.
- [CSSS11] Andrew Cotter, Ohad Shamir, Nati Srebro, and Karthik Sridharan. Better mini-batch algorithms via accelerated gradient methods. In *Advances in neural information processing systems*, pages 1647–1655, 2011.
- [CSX17] Yudong Chen, Lili Su, and Jiaming Xu. Distributed statistical machine learning in adversarial settings: Byzantine gradient descent. *arXiv preprint arXiv:1705.05491*, 2017.
- [DCG16] Sanghamitra Dutta, Viveck Cadambe, and Pulkit Grover. Short-dot: Computing large linear transforms distributedly using coded short dot products. In *Advances In Neural Information Processing Systems*, pages 2100–2108, 2016.
- [DCG17] Sanghamitra Dutta, Viveck Cadambe, and Pulkit Grover. Coded convolution for parallel and distributed computing within a deadline. In *Information Theory (ISIT), 2017 IEEE International Symposium on*, pages 2403–2407. IEEE, 2017.
- [DCM⁺12] Jeffrey Dean, Greg Corrado, Rajat Monga, Kai Chen, Matthieu Devin, Mark Mao, Andrew Senior, Paul Tucker, Ke Yang, Quoc V Le, et al. Large scale distributed deep networks. In *NIPS*, pages 1223–1231, 2012.
- [DPKC11] Lisandro D Dalcin, Rodrigo R Paz, Pablo A Kler, and Alejandro Cosimo. Parallel distributed computing using python. *Advances in Water Resources*, 34(9):1124–1139, 2011.
- [HZRS16] Kaiming He, Xiangyu Zhang, Shaoqing Ren, and Jian Sun. Deep residual learning for image recognition. In *Proceedings of the IEEE conference on computer vision and pattern recognition*, pages 770–778, 2016.
- [JST⁺14] Martin Jaggi, Virginia Smith, Martin Takáč, Jonathan Terhorst, Sanjay Krishnan, Thomas Hofmann, and Michael I Jordan. Communication-efficient distributed dual coordinate ascent. In *NIPS*, pages 3068–3076, 2014.
- [JZ13] Rie Johnson and Tong Zhang. Accelerating stochastic gradient descent using predictive variance reduction. In *Advances in Neural Information Processing Systems*, pages 315–323, 2013.
- [KAD⁺07] Ramakrishna Kotla, Lorenzo Alvisi, Mike Dahlin, Allen Clement, and Edmund Wong. Zyzzyva: speculative byzantine fault tolerance. In *ACM SIGOPS Operating Systems Review*, volume 41, pages 45–58. ACM, 2007.
- [KH09] Alex Krizhevsky and Geoffrey Hinton. Learning multiple layers of features from tiny images. 2009.
- [Kim14] Yoon Kim. Convolutional neural networks for sentence classification. *arXiv preprint arXiv:1408.5882*, 2014.
- [KMR15] Jakub Konečný, Brendan McMahan, and Daniel Ramage. Federated optimization: Distributed optimization beyond the datacenter. *arXiv preprint arXiv:1511.03575*, 2015.
- [KMY⁺16] Jakub Konečný, H Brendan McMahan, Felix X Yu, Peter Richtárik, Ananda Theertha Suresh, and Dave Bacon. Federated learning: Strategies for improving communication efficiency. *arXiv preprint arXiv:1610.05492*, 2016.

- [KSH12] Alex Krizhevsky, Ilya Sutskever, and Geoffrey E Hinton. Imagenet classification with deep convolutional neural networks. In *Advances in neural information processing systems*, pages 1097–1105, 2012.
- [LAP⁺14] Mu Li, David G Andersen, Jun Woo Park, Alexander J Smola, Amr Ahmed, Vanja Josifovski, James Long, Eugene J Shekita, and Bor-Yiing Su. Scaling distributed machine learning with the parameter server. In *OSDI*, volume 14, pages 583–598, 2014.
- [LBBH98] Yann LeCun, Léon Bottou, Yoshua Bengio, and Patrick Haffner. Gradient-based learning applied to document recognition. *Proceedings of the IEEE*, 86(11):2278–2324, 1998.
- [LLP⁺17] Kangwook Lee, Maximilian Lam, Ramtin Pedarsani, Dimitris Papailiopoulos, and Kannan Ramchandran. Speeding up distributed machine learning using codes. *IEEE Transactions on Information Theory*, 2017.
- [LMAA15] Songze Li, Mohammad Ali Maddah-Ali, and A Salman Avestimehr. Coded mapreduce. In *Communication, Control, and Computing (Allerton), 2015 53rd Annual Allerton Conference on*, pages 964–971, 2015.
- [LSP82] Leslie Lamport, Robert Shostak, and Marshall Pease. The byzantine generals problem. *ACM Transactions on Programming Languages and Systems (TOPLAS)*, 4(3):382–401, 1982.
- [LWR⁺14] Ji Liu, Steve Wright, Christopher Re, Victor Bittorf, and Srikrishna Sridhar. An asynchronous parallel stochastic coordinate descent algorithm. In *Proceedings of ICML 14*, pages 469–477, 2014.
- [MPP⁺15] Horia Mania, Xinghao Pan, Dimitris Papailiopoulos, Benjamin Recht, Kannan Ramchandran, and Michael I Jordan. Perturbed iterate analysis for asynchronous stochastic optimization. *NIPS, OPT*, 2015.
- [PGC⁺17] Adam Paszke, Sam Gross, Soumith Chintala, Gregory Chanan, Edward Yang, Zachary DeVito, Zeming Lin, Alban Desmaison, Luca Antiga, and Adam Lerer. Automatic differentiation in pytorch. 2017.
- [PGCC17] Adam Paszke, Sam Gross, Soumith Chintala, and Gregory Chanan. Pytorch, 2017.
- [Pip88] Nicholas Pippenger. Reliable computation by formulas in the presence of noise. *IEEE Transactions on Information Theory*, 34(2):194–197, 1988.
- [PL05] Bo Pang and Lillian Lee. Seeing stars: Exploiting class relationships for sentiment categorization with respect to rating scales. In *Proceedings of the 43rd annual meeting on association for computational linguistics*, pages 115–124. Association for Computational Linguistics, 2005.
- [RPPA17] Amirhossein Reisizadeh, Saurav Prakash, Ramtin Pedarsani, and Salman Avestimehr. Coded computation over heterogeneous clusters. In *Information Theory (ISIT), 2017 IEEE International Symposium on*, pages 2408–2412. IEEE, 2017.
- [RRWN11] Benjamin Recht, Christopher Re, Stephen Wright, and Feng Niu. Hogwild: A lock-free approach to parallelizing stochastic gradient descent. In *NIPS*, pages 693–701, 2011.
- [RTTD17] Netanel Raviv, Itzhak Tamo, Rashish Tandon, and Alexandros G Dimakis. Gradient coding from cyclic mds codes and expander graphs. *arXiv preprint arXiv:1707.03858*, 2017.
- [SLR16] Nihar B Shah, Kangwook Lee, and Kannan Ramchandran. When do redundant requests reduce latency? *IEEE Transactions on Communications*, 64(2):715–722, 2016.
- [SZ14] Karen Simonyan and Andrew Zisserman. Very deep convolutional networks for large-scale image recognition. *arXiv preprint arXiv:1409.1556*, 2014.

- [TLDK17] Rashish Tandon, Qi Lei, Alexandros G Dimakis, and Nikos Karampatziakis. Gradient coding: Avoiding stragglers in distributed learning. In *International Conference on Machine Learning*, pages 3368–3376, 2017.
- [VN56] John Von Neumann. Probabilistic logics and the synthesis of reliable organisms from unreliable components. *Automata studies*, 34:43–98, 1956.
- [ZCL15] Sixin Zhang, Anna E Choromanska, and Yann LeCun. Deep learning with elastic averaging sgd. In *Advances in Neural Information Processing Systems*, pages 685–693, 2015.
- [ZKJ⁺08] Matei Zaharia, Andy Konwinski, Anthony D Joseph, Randy H Katz, and Ion Stoica. Improving mapreduce performance in heterogeneous environments. In *OsdI*, volume 8, page 7, 2008.

A Proofs

A.1 Proof of Theorem 1

For simplicity of proof, let us define a valid s -attack first.

Definition 3. $\mathbf{N} = [\mathbf{n}_1, \mathbf{n}_2, \dots, \mathbf{n}_P]$ is a valid s attack if and only if $|\{j : \|\mathbf{n}_j\|_0 \neq 0\}| \leq s$.

Now we prove theorem 1. Suppose (\mathbf{A}, E, D) can resist s adversaries. The goal is to prove $\|\mathbf{A}\|_0 \geq P(2s + 1)$. In fact we can prove a slightly stronger version: $\|\mathbf{A}_{\cdot, i}\|_0 \geq (2s + 1), i = 1, 2, \dots, B$. Suppose for some $i, \|\mathbf{A}_{\cdot, i}\|_0 = \tau < (2s + 1)$. Without loss of generality, assume that $\mathbf{A}_{1, i}, \mathbf{A}_{2, i}, \dots, \mathbf{A}_{\tau, i}$ are non-zero. Let $\mathbf{G}_{-i} = [\mathbf{g}_1, \mathbf{g}_2, \dots, \mathbf{g}_{i-1}, \mathbf{g}_{i+1}, \dots, \mathbf{g}_P]$. Since (\mathbf{A}, E, D) can protect against s adversaries, we have for any \mathbf{G} ,

$$D(\mathbf{Z}^{\mathbf{A}, E, \mathbf{G}} + \mathbf{N}) = \mathbf{G}\mathbf{1} = \mathbf{G}_{-i}\mathbf{1} + \mathbf{g}_i,$$

for any valid s -attack \mathbf{N} . In particular, let $\mathbf{g}_i^1 = \mathbf{1}_d, \mathbf{g}_i^2 = -\mathbf{1}_d, \mathbf{G}^1 = [\mathbf{g}_1, \mathbf{g}_2, \dots, \mathbf{g}_{i-1}, \mathbf{g}_i^1, \mathbf{g}_{i+1}, \dots, \mathbf{g}_P]$, and $\mathbf{G}^2 = [\mathbf{g}_1, \mathbf{g}_2, \dots, \mathbf{g}_{i-1}, \mathbf{g}_i^2, \mathbf{g}_{i+1}, \dots, \mathbf{g}_P]$. Then for any valid s attack $\mathbf{N}^1, \mathbf{N}^2$,

$$D(\mathbf{Z}^{\mathbf{A}, E, \mathbf{G}^1} + \mathbf{N}^1) = \mathbf{G}_{-i}\mathbf{1}_{P-1} + \mathbf{1}_d.$$

and

$$D(\mathbf{Z}^{\mathbf{A}, E, \mathbf{G}^2} + \mathbf{N}^2) = \mathbf{G}_{-i}\mathbf{1}_{P-1} - \mathbf{1}_d.$$

Our goal is to find $\mathbf{N}^1, \mathbf{N}^2$ such that $D(\mathbf{Z}^{\mathbf{A}, E, \mathbf{G}^1} + \mathbf{N}^1) = D(\mathbf{Z}^{\mathbf{A}, E, \mathbf{G}^2} + \mathbf{N}^2)$ which then will lead to a contradiction. Construct \mathbf{N}^1 and \mathbf{N}^2 by

$$\mathbf{N}_{\ell, j}^1 = \begin{cases} \left[\mathbf{Z}^{\mathbf{A}, E, \mathbf{N}^2} \right]_{\ell, j} - \left[\mathbf{Z}^{\mathbf{A}, E, \mathbf{N}^1} \right]_{\ell, j}, & j = 1, 2, \dots, \lceil \frac{\tau-1}{2} \rceil \\ 0, & \text{otherwise} \end{cases}$$

and

$$\mathbf{N}_{\ell, j}^2 = \begin{cases} \left[\mathbf{Z}^{\mathbf{A}, E, \mathbf{N}^1} \right]_{\ell, j} - \left[\mathbf{Z}^{\mathbf{A}, E, \mathbf{N}^2} \right]_{\ell, j}, & j = \lceil \frac{\tau-1}{2} \rceil, \lceil \frac{\tau-1}{2} \rceil + 1, \dots, \tau \\ 0, & \text{otherwise} \end{cases}$$

One can easily verify that $\mathbf{N}^1, \mathbf{N}^2$ are both valid s attack. Meanwhile, we have

$$\left[\mathbf{Z}^{\mathbf{A}, E, \mathbf{G}^1} \right]_{\ell, j} + \mathbf{N}_{\ell, j}^1 = \left[\mathbf{Z}^{\mathbf{A}, E, \mathbf{G}^2} \right]_{\ell, j} + \mathbf{N}_{\ell, j}^2, j = 1, 2, \dots, \tau$$

due to the above construction of $\mathbf{N}^1, \mathbf{N}^2$. Note that $\mathbf{A}_{j, i} = 0$ for all $j > \tau$, which implies that for all compute nodes with index $j > \tau$, their encoder functions do not depend on the i th gradient. Since \mathbf{G}^1 and \mathbf{G}^2 only differ in the i th gradient, the encoder function of any compute node with index $j > \tau$ should have the same output. Thus, we have

$$\left[\mathbf{Z}^{\mathbf{A}, E, \mathbf{G}^1} \right]_{\ell, j} + \mathbf{N}_{\ell, j}^1 = \left[\mathbf{Z}^{\mathbf{A}, E, \mathbf{G}^1} \right]_{\ell, j} = \left[\mathbf{Z}^{\mathbf{A}, E, \mathbf{G}^2} \right]_{\ell, j} = \left[\mathbf{Z}^{\mathbf{A}, E, \mathbf{G}^2} \right]_{\ell, j} + \mathbf{N}_{\ell, j}^2, j > \tau$$

Hence, we have

$$\left[\mathbf{Z}^{\mathbf{A}, E, \mathbf{G}^1} \right]_{\ell, j} + \mathbf{N}_{\ell, j}^1 = \left[\mathbf{Z}^{\mathbf{A}, E, \mathbf{G}^2} \right]_{\ell, j} + \mathbf{N}_{\ell, j}^2, \forall j$$

which means

$$\mathbf{Z}^{\mathbf{A}, E, \mathbf{G}^1} + \mathbf{N}^1 = \mathbf{Z}^{\mathbf{A}, E, \mathbf{G}^2} + \mathbf{N}^2$$

Therefore, we have

$$D(\mathbf{Z}^{\mathbf{A},E,\mathbf{G}^1} + \mathbf{N}^1) = D(\mathbf{Z}^{\mathbf{A},E,\mathbf{G}^2} + \mathbf{N}^2)$$

and thus

$$\mathbf{G}_{-1}\mathbf{1}_{P-1} + \mathbf{1}_d = D(\mathbf{Z}^{\mathbf{A},E,\mathbf{G}^1} + \mathbf{N}^1) = D(\mathbf{Z}^{\mathbf{A},E,\mathbf{G}^2} + \mathbf{N}^2) = \mathbf{G}_{-1}\mathbf{1}_{P-1} - \mathbf{1}_d$$

This gives us a contradiction. Hence, the assumption is not correct and we must have $\|\mathbf{A}_{\cdot,i}\|_0 \geq (2s+1)$, $i = 1, 2, \dots, P$. Thus, we must have $\|A\|_0 \geq (2s+1)P$. \square

A direct but interesting corollary of this theorem is a bound on the number of adversaries DRACO can resist.

Corollary 6. (\mathbf{A}, E, D) can resist at most $\frac{P-1}{2}$ adversarial nodes.

Proof. According to Theorem 1, the redundancy ratio is at least $2s+1$, meaning that every data point must be replicated by at least $2s+1$. Since there are P compute node in total, we must have $2s+1 \leq P$, which implies $s \leq \frac{P-1}{2}$. Thus, (\mathbf{A}, E, D) can resist at most $\frac{P-1}{2}$ adversaries. \square

In other words, at least a majority of the compute nodes must be non-adversarial. \square

A.2 Proof of Theorem 2

Since there are at most s adversaries, there are at least $2s+1-s = s+1$ non-adversarial compute nodes in each group. Thus, performing majority vote on each group returns the correct gradient, and thus the repetition code guarantees that the result is correct. The complexity at each compute node is clearly $\mathcal{O}((2s+1)d)$ since each of them only computes the sum of $(2s+1)$ d -dimensional gradients. For the decoder at the PS, within each group of $(2s+1)$ machine, it takes $\mathcal{O}((2s+1)d)$ computations to find the majority. Since there are $\frac{P}{(2s+1)}$ groups, it takes in total $\mathcal{O}((2s+1)d\frac{P}{(2s+1)}) = \mathcal{O}(Pd)$ computations. Thus, this achieves linear-time encoding and decoding. \square

A.3 Proof of Lemma 3

We first prove that $\mathbf{A}_{j,k} = 0 \Rightarrow \mathbf{W}_{j,k} = 0$.

Suppose $\mathbf{A}_{j,k} = 0$ for some j, k . Then by definition $k \in \alpha_j$. By $\mathbf{0} = [\mathbf{q}_j \ \mathbf{1}] \cdot [\mathbf{C}_L]_{\cdot, \alpha_j}$ we have $0 = [\mathbf{q}_j \ \mathbf{1}] [\mathbf{C}_L]_{\cdot, k} = \mathbf{W}_{j,k}$.

Next we prove that for any index set U such that $|U| \geq P - (2s+1)$, the column span of $\mathbf{W}_{\cdot, U}$ contains $\mathbf{1}$. This is equivalent to that for any index set U such that $|U| \geq P - (2s+1)$, there exists a vector \mathbf{b} such that $\mathbf{W}_{\cdot, U}\mathbf{b} = \mathbf{1}$. Now we show such \mathbf{b} exists. Note that \mathbf{C}_L is a $(P-2s) \times P$ full rank Vandermonde matrix and thus any $P-2s$ columns of \mathbf{C}_L are linearly independent. Let \bar{U} be the first $P-2s$ elements in U . Then all columns of $[\mathbf{C}_L]_{\cdot, \bar{U}}$ are linearly independent and thus $[\mathbf{C}_L]_{\cdot, \bar{U}}$ is invertible. Let $\mathbf{b}_{\bar{U}} \triangleq \bar{\mathbf{b}} = (\mathbf{C}_{\bar{U}}^L)^{-1} [0 \ 0 \ \dots \ 0 \ 1]^T$. For any $j \notin \bar{U}$, let $\mathbf{b}_j = 0$. Then we have

$$\begin{aligned} \mathbf{W}_U \mathbf{b} &= [\mathbf{Q} \ \mathbf{1}] \times [\mathbf{C}_L]_{\cdot, U} \mathbf{b} \\ &= [\mathbf{Q} \ \mathbf{1}] \times [\mathbf{C}_L]_{\cdot, \bar{U}} \bar{\mathbf{b}} \\ &= [\mathbf{Q} \ \mathbf{1}] \times [\mathbf{C}_L]_{\cdot, \bar{U}} \times [\mathbf{C}_L]_{\cdot, \bar{U}}^{-1} [0 \ 0 \ \dots \ 0 \ 1]^T \\ &= [\mathbf{Q} \ \mathbf{1}] [0 \ 0 \ \dots \ 0 \ 1]^T \\ &= \mathbf{1}. \end{aligned}$$

This completes the proof. \square

A.4 Proof of Lemma 4

We need a few lemmas first.

Lemma 7. Let a P -dimensional vector $\boldsymbol{\gamma} \triangleq [\gamma_1, \gamma_2, \dots, \gamma_P]^T = (\mathbf{f}\mathbf{N})^T$. Then we have

$$\Pr(\{j : \gamma_j \neq 0\} = \{j : \|\mathbf{N}_{\cdot,j}\|_0 \neq 0\}) = 1.$$

Proof. Let us prove that

$$\Pr(\mathbf{N}_{\cdot,j} \neq 0 | \gamma_j \neq 0) = 1.$$

and

$$\Pr(\gamma_j \neq 0 | \mathbf{N}_{\cdot,j} \neq 0) = 1.$$

for any j . Combining those two equations we prove the lemma.

The first equation is straightforward. Suppose $\mathbf{N}_{\cdot,j} = 0$. Then we immediately have $\gamma_j = \mathbf{f}\mathbf{N}_{\cdot,j} = 0$. For the second one, note that \mathbf{f} has entries drawn independently from the standard normal distribution. Therefore we have that $\gamma_j = \mathbf{f}\mathbf{N}_{\cdot,j} \sim \mathcal{N}(\mathbf{1}^T \mathbf{N}_{\cdot,j}, \|\mathbf{N}_{\cdot,j}\|_2^2)$. Since γ_j is a random variable with normal distribution, the probability of it being any particular value is 0. In particular,

$$\Pr(\gamma_j = 0 | \mathbf{N}_{\cdot,j} \neq 0) = 0,$$

and thus

$$\Pr(\gamma_j \neq 0 | \mathbf{N}_{\cdot,j} \neq 0) = 1$$

which proves the second equation and finishes the proof. \square

Lemma 8. $\mathbf{R}^{Cyc} \mathbf{C}_R^\dagger = \mathbf{N} \mathbf{C}_R^\dagger$.

Proof. By definition, $\mathbf{R}^{Cyc} \mathbf{C}_R^\dagger = (\mathbf{G}\mathbf{W} + \mathbf{N}) \mathbf{C}_R^\dagger = (\mathbf{G}[\mathbf{Q} \ \mathbf{1}] \mathbf{C}_L + \mathbf{N}) \mathbf{C}_R^\dagger = \mathbf{G}[\mathbf{Q} \ \mathbf{1}] \mathbf{C}_L \mathbf{C}_R^\dagger + \mathbf{N} \mathbf{C}_R^\dagger = \mathbf{N} \mathbf{C}_R^\dagger$. In the last equation we use the fact that IDFT matrix is unitary and thus $\mathbf{C}_L \mathbf{C}_R^\dagger = \mathbf{0}_{(P-2s) \times (2s)}$. \square

Lemma 9. Let a P -dimensional vector $\hat{\mathbf{h}} \triangleq [\hat{h}_0, \hat{h}_1, \dots, \hat{h}_{P-1}]^T$ be the discrete Fourier transformation (DFT) of a P -dimensional vector $\hat{\mathbf{t}} \triangleq [\hat{t}_1, \hat{t}_2, \dots, \hat{t}_{P-1}]^T$ which has at most s non-zero elements, i.e., $\hat{\mathbf{h}} = \mathbf{C}^\dagger \hat{\mathbf{t}}$ and $\|\hat{\mathbf{t}}\|_0 \leq s$. Then there exists a s -dimensional vector $\hat{\boldsymbol{\beta}} \triangleq [\hat{\beta}_0, \hat{\beta}_1, \dots, \hat{\beta}_{s-1}]^T$, such that

$$\begin{bmatrix} \hat{h}_{P-s-1} & \hat{h}_{P-s} & \dots & \hat{h}_{P-2} \\ \hat{h}_{P-s-2} & \hat{h}_{P-s-1} & \dots & \hat{h}_{P-3} \\ \dots & \dots & \ddots & \vdots \\ \hat{h}_{P-2s} & \hat{h}_{P-s+1} & \dots & \hat{h}_{P-s-1} \end{bmatrix} \hat{\boldsymbol{\beta}} = \begin{bmatrix} \hat{h}_{P-1} \\ \hat{h}_{P-2} \\ \vdots \\ \hat{h}_{P-s} \end{bmatrix}. \quad (\text{A.1})$$

Furthermore, for any $\hat{\boldsymbol{\beta}}$ satisfying the above equations,

$$\hat{h}_\ell = \sum_{u=0}^{s-1} \hat{\beta}_u \hat{h}_{\ell+u-s}, \quad (\text{A.2})$$

always holds for all ℓ , where $\hat{h}_\ell = \hat{h}_{P+\ell}$.

Proof. Let i_1, i_2, \dots, i_s be the index of the non-zero elements in $\hat{\mathbf{t}}$. Let us define the location polynomial $p(\omega) = \prod_{k=1}^s (\omega - e^{-\frac{2\pi i}{P} i_k}) \triangleq \sum_{k=0}^s \theta_k \omega^k$, where $\theta_s = 1$. Let a s -dimensional vector $\hat{\beta}^* \triangleq -[\theta_0, \theta_1, \dots, \theta_{s-1}]^T$.

Now we prove that $\hat{\beta} = \hat{\beta}^*$ is a solution to the system of linear equations (A.1). To see this, note that by definition, for any λ , we have $0 = p(e^{-\frac{2\pi i}{P} i_\lambda}) = \sum_{k=0}^s \theta_k e^{-\frac{2\pi i}{P} i_\lambda k}$. Multiply both side by $\hat{t}_{i_\lambda} e^{-\frac{2\pi i}{P} i_\lambda \eta}$, we have

$$\begin{aligned} 0 &= \hat{t}_{i_\lambda} e^{-\frac{2\pi i}{P} i_\lambda \eta} \sum_{k=0}^s \theta_k e^{-\frac{2\pi i}{P} i_\lambda k} \\ &= \hat{t}_{i_\lambda} \sum_{k=0}^s \theta_k e^{-\frac{2\pi i}{P} i_\lambda (k+\eta)}. \end{aligned}$$

Summing over λ , we have

$$\begin{aligned} 0 &= \sum_{\lambda=1}^s \hat{t}_{i_\lambda} \sum_{k=0}^s \theta_k e^{-\frac{2\pi i}{P} i_\lambda (k+\eta)} \\ &= \sum_{k=0}^s \theta_k \sum_{\lambda=1}^s \hat{t}_{i_\lambda} e^{-\frac{2\pi i}{P} i_\lambda (k+\eta)}. \end{aligned}$$

By definition, $\hat{h}_j = \mathbf{C}_j \cdot \hat{\mathbf{t}} = \frac{1}{\sqrt{P}} \sum_{k=0}^{P-1} e^{-\frac{2\pi i}{P} jk} \hat{t}_k = \frac{1}{\sqrt{P}} \sum_{\lambda=1}^s \hat{t}_{i_\lambda} e^{-\frac{2\pi i}{P} i_\lambda j}$. Hence, the above equation becomes

$$0 = \sum_{k=0}^s \theta_k \sqrt{P} \hat{h}_{k+\eta}$$

which is equivalent to

$$\hat{h}_{s+\eta} = \sum_{k=0}^{s-1} -\theta_k \hat{h}_{k+\eta}$$

due to the fact that $\theta_s = 1$. By setting $\eta = -s + P - 1, -s + P - 2, \dots, -s + P - s$, one can easily see that the above equation becomes identical to the system of linear equations in (A.1) with $\hat{\beta} = \hat{\beta}^* = -[\theta_0, \theta_1, \dots, \theta_{s-1}]^T$.

Now let us prove for any $\hat{\beta}$ that satisfies equation (A.1), we have (A.2). Note that an equivalent form of (A.2) is that the following system of linear equations

$$\begin{bmatrix} \hat{h}_{P-s-1+\ell} & \hat{h}_{P-s+\ell} & \dots & \hat{h}_{P-2+\ell} \\ \hat{h}_{P-s-2+\ell} & \hat{h}_{P-s-1+\ell} & \dots & \hat{h}_{P-3+\ell} \\ \dots & \dots & \ddots & \vdots \\ \hat{h}_{P-2s+\ell} & \hat{h}_{P-s+1+\ell} & \dots & \hat{h}_{P-s-1+\ell} \end{bmatrix} \hat{\beta} = \begin{bmatrix} \hat{h}_{P-1+\ell} \\ \hat{h}_{P-2+\ell} \\ \vdots \\ \hat{h}_{P-s+\ell} \end{bmatrix} \quad (\text{A.3})$$

holds for $\ell = 0, 1, 2, \dots, P-1$. We prove this by induction. When $\ell = 1$, this is true since $\hat{\beta}$ satisfies the system of linear equations in (A.1). Assume it holds for $\ell = \mu$, i.e.,

$$\begin{bmatrix} \hat{h}_{P-s-1+\mu} & \hat{h}_{P-s+\mu} & \dots & \hat{h}_{P-2+\mu} \\ \hat{h}_{P-s-2+\mu} & \hat{h}_{P-s-1+\mu} & \dots & \hat{h}_{P-3+\mu} \\ \dots & \dots & \ddots & \vdots \\ \hat{h}_{P-2s+\mu} & \hat{h}_{P-s+1+\mu} & \dots & \hat{h}_{P-s-1+\mu} \end{bmatrix} \hat{\beta} = \begin{bmatrix} \hat{h}_{P-1+\mu} \\ \hat{h}_{P-2+\mu} \\ \vdots \\ \hat{h}_{P-s+\mu} \end{bmatrix}$$

Now we need to prove it also holds when $\ell = \mu + 1$, i.e.,

$$\begin{bmatrix} \hat{h}_{P-s-1+\mu+1} & \hat{h}_{P-s+\mu+1} & \cdots & \hat{h}_{P-2+\mu+1} \\ \hat{h}_{P-s-2+\mu+1} & \hat{h}_{P-s-1+\mu+1} & \cdots & \hat{h}_{P-3+\mu+1} \\ \cdots & \cdots & \ddots & \vdots \\ \hat{h}_{P-2s+\mu+1} & \hat{h}_{P-s+1+\mu+1} & \cdots & \hat{h}_{P-s-1+\mu+1} \end{bmatrix} \hat{\beta} = \begin{bmatrix} \hat{h}_{P-1+\mu+1} \\ \hat{h}_{P-2+\mu+1} \\ \vdots \\ \hat{h}_{P-s+\mu+1} \end{bmatrix}.$$

First, since both $\hat{\beta}, \hat{\beta}^*$ satisfy the induction assumption, we must have

$$\begin{bmatrix} \hat{h}_{P-s-1+\mu} & \hat{h}_{P-s+\mu} & \cdots & \hat{h}_{P-2+\mu} \\ \hat{h}_{P-s-2+\mu} & \hat{h}_{P-s-1+\mu} & \cdots & \hat{h}_{P-3+\mu} \\ \cdots & \cdots & \ddots & \vdots \\ \hat{h}_{P-2s+\mu} & \hat{h}_{P-s+1+\mu} & \cdots & \hat{h}_{P-s-1+\mu} \end{bmatrix} (\hat{\beta} - \hat{\beta}^*) = \mathbf{0}_s.$$

Due to the induction assumption, one can verify that

$$[\theta_{s-1}, \theta_{s-2}, \cdots, \theta_0] \begin{bmatrix} \hat{h}_{P-s-1+\mu} & \hat{h}_{P-s+\mu} & \cdots & \hat{h}_{P-2+\mu} \\ \hat{h}_{P-s-2+\mu} & \hat{h}_{P-s-1+\mu} & \cdots & \hat{h}_{P-3+\mu} \\ \cdots & \cdots & \ddots & \vdots \\ \hat{h}_{P-2s+\mu} & \hat{h}_{P-s+1+\mu} & \cdots & \hat{h}_{P-s-1+\mu} \end{bmatrix} = [\hat{h}_{P-s+\mu} \quad \hat{h}_{P-s+\mu+1} \quad \cdots \quad \hat{h}_{P-2+\mu+1}],$$

and thus we have

$$\begin{aligned} & [\hat{h}_{P-s+\mu} \quad \hat{h}_{P-s+\mu+1} \quad \cdots \quad \hat{h}_{P-2+\mu+1}] (\hat{\beta} - \hat{\beta}^*) \\ &= [\theta_{s-1}, \theta_{s-2}, \cdots, \theta_0] \begin{bmatrix} \hat{h}_{P-s-1+\mu} & \hat{h}_{P-s+\mu} & \cdots & \hat{h}_{P-2+\mu} \\ \hat{h}_{P-s-2+\mu} & \hat{h}_{P-s-1+\mu} & \cdots & \hat{h}_{P-3+\mu} \\ \cdots & \cdots & \ddots & \vdots \\ \hat{h}_{P-2s+\mu} & \hat{h}_{P-s+1+\mu} & \cdots & \hat{h}_{P-s-1+\mu} \end{bmatrix} (\hat{\beta} - \hat{\beta}^*) = 0. \end{aligned}$$

Hence,

$$\begin{aligned} & [\hat{h}_{P-s+\mu} \quad \hat{h}_{P-s-1+\mu} \quad \cdots \quad \hat{h}_{P-1+\mu}] \hat{\beta} \\ &= [\hat{h}_{P-s+\mu} \quad \hat{h}_{P-s-1+\mu} \quad \cdots \quad \hat{h}_{P-1+\mu}] \hat{\beta}^* + [\hat{h}_{P-s+\mu} \quad \hat{h}_{P-s-1+\mu} \quad \cdots \quad \hat{h}_{P-1+\mu}] (\hat{\beta} - \hat{\beta}^*) = \hat{h}_{P+\mu} = \hat{h}_{P-1+\mu+1}. \end{aligned}$$

Furthermore, by induction assumption, we have

$$\begin{aligned} & \begin{bmatrix} \hat{h}_{P-s-2+\mu+1} & \hat{h}_{P-s-1+\mu+1} & \cdots & \hat{h}_{P-3+\mu+1} \\ \hat{h}_{P-s-3+\mu+1} & \hat{h}_{P-s-2+\mu+1} & \cdots & \hat{h}_{P-4+\mu+1} \\ \cdots & \cdots & \ddots & \vdots \\ \hat{h}_{P-2s+\mu+1} & \hat{h}_{P-s+1+\mu+1} & \cdots & \hat{h}_{P-s+1+\mu+1} \end{bmatrix} \hat{\beta} = \begin{bmatrix} \hat{h}_{P-s-1+\mu} & \hat{h}_{P-s-2+\mu} & \cdots & \hat{h}_{P-2+\mu} \\ \hat{h}_{P-s-2+\mu} & \hat{h}_{P-s-1+\mu} & \cdots & \hat{h}_{P-3+\mu} \\ \cdots & \cdots & \ddots & \vdots \\ \hat{h}_{P-(2s-1)+\mu} & \hat{h}_{P-s+\mu} & \cdots & \hat{h}_{P-s+\mu} \end{bmatrix} \hat{\beta} \\ &= \begin{bmatrix} \hat{h}_{P-1+\mu} \\ \hat{h}_{P-2+\mu} \\ \vdots \\ \hat{h}_{P-(s-1)+\mu} \end{bmatrix} = \begin{bmatrix} \hat{h}_{P-2+(\mu+1)} \\ \hat{h}_{P-3+(\mu+1)} \\ \vdots \\ \hat{h}_{P-s+(\mu+1)} \end{bmatrix}. \end{aligned}$$

Combing those two result we have proved

$$\begin{bmatrix} \hat{h}_{P-s-1+\mu+1} & \hat{h}_{P-s+\mu+1} & \cdots & \hat{h}_{P-2+\mu+1} \\ \hat{h}_{P-s-2+\mu+1} & \hat{h}_{P-s-1+\mu+1} & \cdots & \hat{h}_{P-3+\mu+1} \\ \cdots & \cdots & \ddots & \vdots \\ \hat{h}_{P-2s+\mu+1} & \hat{h}_{P-s+1+\mu+1} & \cdots & \hat{h}_{P-s-1+\mu+1} \end{bmatrix} \hat{\beta} = \begin{bmatrix} \hat{h}_{P-1+\mu+1} \\ \hat{h}_{P-2+\mu+1} \\ \vdots \\ \hat{h}_{P-s+\mu+1} \end{bmatrix}.$$

By induction, the equation A.3 holds for all $\ell = 0, 1, \dots, P-1$. Equation A.3 immediately finishes the proof. \square

Now we are ready to prove Lemma 4. By Lemma 7, for the P -dimensional vector $\gamma = (\mathbf{fN})^T$, we have

$$Pr(\{j : \gamma_j \neq 0\} = \{j : \|\mathbf{N}_{\cdot,j}\|_0 \neq 0\}) = 1,$$

Since there are at most s adversaries, the number of non-zero columns in \mathbf{N} is at most s and hence there are at most s non-zero elements in γ , i.e., $\|\gamma\|_0 \leq s$, with probability 1. Now consider the case when $\|\gamma\|_0 \leq s$. First note that $[h_{P-2s}, h_{P-2s+1}, \dots, h_{P-1}] = \mathbf{fR}^{Cyc}\mathbf{C}_R^\dagger = \mathbf{fN}\mathbf{C}_R^\dagger = \gamma^T\mathbf{C}_{R'}^\dagger$, where the second equation is due to Lemma 8. Now let us construct $\hat{\mathbf{h}} = [\hat{h}_0, \hat{h}_1, \dots, \hat{h}_{P-1}]^T$ by $\hat{\mathbf{h}} = \mathbf{C}^\dagger\gamma$. Note that \mathbf{C} is symmetric and thus $\mathbf{C}^\dagger = [\mathbf{C}^\dagger]^T$. One can easily verify that $\hat{h}_\ell = h_\ell, \ell = P-2s, P-2s+1, \dots, P-1$. Therefore, the equation

$$\begin{bmatrix} h_{P-s-1} & h_{P-s} & \dots & h_{P-2} \\ h_{P-s-2} & h_{P-s-1} & \dots & h_{P-3} \\ \dots & \dots & \ddots & \vdots \\ h_{P-2s} & h_{P-s+1} & \dots & h_{P-s+1} \end{bmatrix} \begin{bmatrix} \beta_0 \\ \beta_1 \\ \vdots \\ \beta_{s-1} \end{bmatrix} = \begin{bmatrix} h_{P-1} \\ h_{P-2} \\ \vdots \\ h_{P-s} \end{bmatrix}$$

becomes

$$\begin{bmatrix} \hat{h}_{P-s-1} & h_{P-s} & \dots & \hat{h}_{P-2} \\ \hat{h}_{P-s-2} & \hat{h}_{P-s-1} & \dots & \hat{h}_{P-3} \\ \dots & \dots & \ddots & \vdots \\ \hat{h}_{P-2s} & \hat{h}_{P-s+1} & \dots & \hat{h}_{P-s+1} \end{bmatrix} \begin{bmatrix} \beta_0 \\ \beta_1 \\ \vdots \\ \beta_{s-1} \end{bmatrix} = \begin{bmatrix} \hat{h}_{P-1} \\ \hat{h}_{P-2} \\ \vdots \\ \hat{h}_{P-s} \end{bmatrix}$$

which always has a solution. Assume we find one solution $\bar{\beta} = [\bar{\beta}_0, \bar{\beta}_1, \dots, \bar{\beta}_{P-1}]^T$. By the second part of Lemma 9, we have

$$\hat{h}_\ell = \sum_{u=0}^{s-1} \bar{\beta}_u \hat{h}_{\ell+u-s}, \forall \ell.$$

Now we prove by induction that $h_\ell = \hat{h}_\ell, \ell = 0, 1, \dots, P-1$.

When $\ell = 0$, we have

$$\hat{h}_0 = \sum_{u=0}^{s-1} \bar{\beta}_u \hat{h}_{u-s} = \sum_{u=0}^{s-1} \bar{\beta}_u h_{u-s} = h_0$$

where the second equation is due to the fact that $[h_{P-2s}, h_{P-2s-1}, \dots, h_{P-1}] = [\hat{h}_{P-2s}, \hat{h}_{P-2s-1}, \dots, \hat{h}_{P-1}]$ and $\hat{h}_{P+\ell} = \hat{h}_\ell, h_{P+\ell} = h_\ell$ (by definition).

Assume that for $\ell \leq \mu, \hat{h}_\ell = h_\ell$.

When $\ell = \mu + 1$, we have

$$\hat{h}_{\mu+1} = \sum_{u=0}^{s-1} \bar{\beta}_u \hat{h}_{\mu+1+u-s} = \sum_{u=0}^{s-1} \bar{\beta}_u h_{\mu+1+u-s} = h_{\mu+1}$$

where the second equation is because of the induction assumption for $\ell \leq \mu, \hat{h}_\ell = h_\ell$.

Thus, we have $h_\ell = \hat{h}_\ell$ for all ℓ , which means $\mathbf{h} = \hat{\mathbf{h}} = \mathbf{C}^\dagger\gamma$. Thus \mathbf{t} , the IDFT of \mathbf{h} , becomes $\mathbf{t} = \mathbf{C}\mathbf{h} = \mathbf{C}\mathbf{C}^\dagger\gamma = \gamma$. Then the returned Index Set $V = \{j : e_{j+1} \neq 0\} = \{j : \gamma_j \neq 0\}$. By Lemma 7, with probability 1, $\{j : \gamma_j \neq 0\} = \{j : \|\mathbf{n}_j\|_0 \neq 0\}$. Therefore, we have with probability 1, $V = \{j : \|\mathbf{n}_j\|_0 \neq 0\}$, which finishes the proof. \square

A.5 Proof of Theorem 5

We first prove the correctness of the cyclic code. By Lemma 4, the set U contains the index of all non-adversarial compute nodes with probability 1. By Lemma 3, there exists \mathbf{b} such that $\mathbf{W}_{\cdot,U}\mathbf{b} = \mathbf{1}$. Therefore, $\mathbf{u}^{Cyc} = \mathbf{R}_{\cdot,U}^{Cyc}\mathbf{b} = (\mathbf{GW} + \mathbf{N})_{\cdot,U}\mathbf{b} = \mathbf{GW}_{\cdot,U}\mathbf{b} = \mathbf{G}\mathbf{1}_P$. Thus, The cyclic code $(\mathbf{A}^{Cyc}, E^{Cyc}, D^{Cyc})$ can recover the desired gradient and hence resist any $\leq s$ adversaries with probability 1.

Next we show the efficiency of the cyclic code. By the construction of \mathbf{A}^{Cyc} and \mathbf{W} , the redundancy ratio is $2s + 1$ which reaches the lower bound. Each compute node needs to compute a linear combination of the gradients of the data it holds, which needs $\mathcal{O}((2s + 1)d)$ computations. For the PS, the detection function $\phi(\cdot)$ takes $\mathcal{O}(d)$ (generating the random vector \mathbf{f}) + $\mathcal{O}(dP + 2Ps)$ (computing \mathbf{fRC}_R^\dagger) + $\mathcal{O}(s^2)$ (solving the Toeplitz system of linear equations in (A.1)) + $\mathcal{O}((P - 2s)s)$ (computing $h_\ell, \ell = 0, 1, 2, \dots, P - 2s - 1$) + $\mathcal{O}(P \log P)$ (computing the DFT of \mathbf{h}) + $\mathcal{O}(P)$ (examining the non-zero elements of \mathbf{t}) = $\mathcal{O}(d + dP + 2Ps + s^2 + (P - 2s)s + P \log P + P) = \mathcal{O}(dP + Ps + P \log P)$. Finding the vector \mathbf{b} takes $\mathcal{O}(P^3)$ (by simply constructing \mathbf{b} via $[\mathbf{C}_L]_{\cdot,U}$, though better algorithms may exist). The recovering equation $\mathbf{R}_{\cdot,U}\mathbf{b}$ takes $\mathcal{O}(dP)$. Thus, in total, the decoder at the PS takes $\mathcal{O}(dP + P^3 + P \log P)$. When $d \gg P$, i.e., $d = \Omega(P^2)$, this becomes $\mathcal{O}(dP)$. Therefore, $(\mathbf{A}^{Cyc}, E^{Cyc}, D^{Cyc})$ also achieves linear-time encoding and decoding. \square

B Streaming Majority Vote Algorithm

In this section we present the Boyer—Moore majority vote algorithm [BM91], which is an algorithm that only needs computation linear in the size of the sequence.

Algorithm 2 Streaming Majority Vote.

Input : n items I_1, I_2, \dots, I_n

Output: The majority of the n items

Initialize an element $Ma = I_1$ and a counter $Counter = 0$.

```

for  $i = 1$  to  $n$  do
  if  $Counter == 0$  then
     $Ma = I_i$ .
     $Counter = 1$ .
  else if  $Ma == I_i$  then
     $Counter = Counter + 1$ .
  else
     $Counter = Counter - 1$ .
  end

```

end

Return Ma .

Clearly this algorithm runs in linear time and it is known that if there is a majority item then the algorithm finally will return it [BM91].